Circulation Research
JOURNAL OF THE AMERICAN HEART ASSOCIATION

Acute Depletion of Endothelial β3-Integrin Transiently Inhibits Tumor Growth and Angiogenesis in Mice

Veronica Steri, Tim S. Ellison, Aleksander Maksym Gontarczyk, Katherine Weilbaecher, Jochen G. Schneider, Dylan Edwards, Marcus Fruttiger, Kairbaan M. Hodivala-Dilke and Stephen Douglas Robinson

Circ Res. 2014;114:79-91; originally published online October 8, 2013;
doi: 10.1161/CIRCRESAHA.114.301591
Circulation Research is published by the American Heart Association, 7272 Greenville Avenue, Dallas, TX 75231

Print ISSN: 0009-7330. Online ISSN: 1524-4571

Acute Depletion of Endothelial β3-Integrin Transiently Inhibits Tumor Growth and Angiogenesis in Mice

Veronica Steri, Tim S. Ellison, Aleksander Maksym Gontarczyk, Katherine Weilbaecher, Jochen G. Schneider, Dylan Edwards, Marcus Fruttiger, Kairbaan M. Hodivala-Dilke, Stephen Douglas Robinson

Rationale: **The dramatic upregulation of αvβ3-integrin that occurs in the vasculature during tumor growth has long suggested that the endothelial expression of this molecule is an ideal target for antiangiogenic therapy to treat cancer. This discovery led to the development of small-molecule inhibitors directed against αvβ3-integrin that are currently in clinical trials. In 2002, we reported that β3-integrin–knockout mice exhibit enhanced tumor growth and angiogenesis. However, as β3-integrin is expressed by a wide variety of cells, endothelial cell–specific contributions to tumor angiogenesis are muddied by the use of a global knockout of β3-integrin function.**

Objective: **Our aim was to examine the endothelial-specific contribution β3-integrin makes to tumor growth and angiogenesis.**

Methods and Results: **We have crossed β3-integrin–floxed (β3-floxed) mice to 2 endothelial-specific Cre models and examined angiogenic responses in vivo, ex vivo, and in vitro. We show that acute depletion of endothelial β3-integrin inhibits tumor growth and angiogenesis preventatively, but not in already established tumors. However, the effects are transient, and long-term depletion of the molecule is ineffective. Furthermore, long-term depletion of the molecule correlates with many molecular changes, such as reduced levels of focal adhesion kinase expression and a misbalance in focal adhesion kinase phosphorylation, which may lead to a release from the inhibitory effects of decreased endothelial β3-integrin expression.**

Conclusions: **Our findings imply that timing and length of inhibition are critical factors that need to be considered when targeting the endothelial expression of β3-integrin to inhibit tumor growth and angiogenesis. (*Circ Res*. 2014;114:79-91.)**

Key Words: angiogenesis inhibitors ■ endothelium ■ integrin αVβ3 ■ neoplasms

In order to grow and metastasize, solid tumors must recruit their own blood supply from the surrounding vasculature. This process, called angiogenesis, is initiated when the hypoxic tumor begins to release angiogenic growth factors, such as vascular endothelial growth factor (VEGF). New blood vessel formation follows in a step-wise fashion with the removal of supporting cells (pericytes) from the existing nearby capillary vasculature and the degradation of the endothelial cell basement membrane and extracellular matrix. Endothelial cells begin to proliferate and migrate toward the tumor. These latter processes are dependent on integrins.[1]

Editorial, see p 9

Integrins are heterodimeric transmembrane extracellular matrix receptors composed of an α- and a β-subunit.[2] αvβ3-Integrin is expressed by endothelial cells on stimulation with angiogenic growth factors, and its expression is dramatically upregulated in tumor vasculature at sites of inflammation and tissue repair.[3–5] Ligation of αvβ3-integrin induces endothelial cell proliferation, survival, and migration. In addition, αvβ3-integrin and VEGF receptor 2 (VEGFR2) interact synergistically in endothelial cells to promote angiogenesis.[6] These findings indicate a proangiogenic role for αvβ3-integrin, which correlates with its enhanced expression by tumor vasculature. As such, αvβ3-integrin has become an attractive antiangiogenic target for the development of antagonists. β3-Integrin blockade using antibodies, Arg-Gly-Asp (RGD) peptide antagonists, or signaling-defective mutants results in reduced tumor growth and angiogenesis.[4,7–9]

In contrast, however, genetic ablation studies suggest an antiangiogenic role for αvβ3-integrin. β3-Integrin–knockout mice exhibit enhanced tumor growth and angiogenesis that is

Original received April 14, 2013; revision received October 4, 2013; accepted October 8, 2013. In September 2013, the average time from submission to first decision for all original research papers submitted to *Circulation Research* was 13.2 days.

From the School of Biological Sciences, University of East Anglia, Norwich Research Park, Norwich, United Kingdom (V.S., T.S.E., A.M.G., D.E., S.D.R.); Department of Internal Medicine, Division of Molecular Oncology, Washington University in St Louis, MO (K.W.); Luxembourg Center for Systems Biomedicine, University of Luxembourg, Luxembourg and Saarland University Medical Center, Internal Medicine II, Homburg, Germany (J.G.S.); UCL Institute of Ophthalmology, University College London, London, United Kingdom (M.F.); Barts Cancer Institute - a Cancer Research UK Centre of Excellence, Queen Mary, University of London, John Vane Science Centre, Charterhouse Square, London, United Kingdom (K.M.H.-D.).

Correspondence to Stephen D. Robinson, PhD, School of Biological Sciences, University of East Anglia, Norwich Research Park, Norwich NR4 7TJ, United Kingdom. E-mail stephen.robinson@uea.ac.uk

Circulation Research **is available at http://circres.ahajournals.org** **DOI: 10.1161/CIRCRESAHA.114.301591**

Nonstandard Abbreviations and Acronyms	
BMDC	bone marrow derived cell
FAK	focal adhesion kinase
LuEC	lung microvascular endothelial cell
OHT	4-hydroxy-tamoxifen
VEGFR2	vascular endothelial growth factor (VEGF) receptor 2

associated with an upregulation of VEGFR2 expression and signaling.[10,11] Furthermore, β3-integrin expression limits the contribution that neuropilin-1 (a VEGF coreceptor) makes to VEGF-induced angiogenesis, thereby inhibiting the process.[12]

Based on knockout and inhibition studies, a combination of pro- and antiangiogenic roles have been assigned to β3-integrin. One limitation of both approaches is, however, the global level at which the analyses have taken place. β3-Integrin expression is not restricted to neovascular endothelial cells. It is expressed on platelets and megakaryocytes (where it plays a critical role in platelet aggregation) and by pericytes and bone marrow–derived cells (BMDCs), all of which may contribute to angiogenesis (see Robinson and Hodivala-Dilke[13] for a recent review). Bone marrow transplantation studies, for example, have clearly demonstrated that the absence of β3-integrin expression in BMDCs in β3-integrin–knockout animals contributes to the enhanced tumor growth in this model.[14,15]

We present here a dissection of the contribution made specifically by endothelial β3-integrin to tumor growth and angiogenesis. The knowledge gained from these studies is key to understanding the basic biology behind the dramatic vascular upregulation of this molecule during neoangiogeneis and, more impotantly, to improving the design of therapeutic strategies that target the expression of the molecule. The current strategies have proven to be somewhat disappointing with many tumors either not responding to or becoming resistant to β3-integrin–directed therapy.[16] Because this is of such fundamental importance, we have re-evaluated the function of β3-integrin in tumor angiogenesis by crossing β3-floxed mice[17] to 2 different endothelial-specific Cre lines—lines we have used separately in the past to elucidate the role of other endothelial integrins[18,19] and focal adhesion kinase (FAK)[20] in tumor angiogenesis. Tie1Cre[21] constitutively depletes floxed targets in endothelial cells, thereby creating a cell-specific mimic of a global knockout, whereas Pdgfb-iCreER^{T2} (see Claxton et al[22]) depletes floxed targets in endothelial cells in a 4-hydroxy-tamoxifen (OHT)-inducible fashion (a model more akin to antagonist administration). We have used these mice to analyze growth and angiogenesis in subcutaneous syngeneic tumor models, as well as in ex vivo and in vitro angiogenic assays.

Methods

Animals

A detailed description of the mice used in this study can be found in the Methods section in the Online Data Supplement. All animals were on a mixed C57BL6/129 background. Littermate controls were used for all in vivo experiments. All animal experiments were performed in accordance with UK Home Office regulations and the European Legal Framework for the protection of animals used for scientific purposes (European Directive 86/609/EEC).

In Vivo Tumor Growth Assay

Syngeneic mouse tumor cell lines, B16F0 (melanoma, derived from C57BL6) and CMT19T (lung carcinoma, derived from C57BL6), were used in subcutaneous tumor growth experiments as described elsewhere.[20] Detailed parameters can be found in the Online Data Supplement.

Immunohistochemical Analysis

Histological analyses were performed as described previously.[23] Antibodies used and detailed staining parameters can be found in the Online Data Supplement.

Mouse Tumor Endothelial Cell Isolation

PECAM1-positive cells were isolated from enzymatically digested tumors by magnetic activated cell sorting. Detailed parameters can be found in the Online Data Supplement.

Mouse Lung Endothelial Cell Isolation and Culture

Lung microvascular endothelial cells (LuECs) were isolated and cultured as described elsewhere.[12] Detailed parameters can be found in the Online Data Supplement.

Ex Vivo Aortic Ring Assays

Thoracic aortae were isolated from 6- to 9-week-old adult mice and prepared for culture as described previously.[24] VEGF assays were performed in collagen, fibroblast growth factor assays in fibrin. Where indicated, VEGF or fibroblast growth factor was added at 30 ng/mL. Microvessel growth on aortic rings was quantified after 6 to 10 days. After maximum sprouting capacity was achieved, aortic rings were fixed and stained with FITC-IB4 lectin and visualized by epifluorescence.

Bone Marrow Isolation

BMDCs were isolated by flushing femurs of β3-floxed/Tie1Cre-negative/positive animals or from 15-day, OHT-treated β3-floxed/Pdgfb-iCreER^{T2}-negative/positive mice with PBS. Cells were passed through a 70-μm mesh and collected by centrifugation at 1500 rpm for 5 minutes. Red blood cells were lyzed in Red Blood Lysis buffer (eBioscience) for 5 minutes. Cells were resupended in PBS containing 1% fetal bovine serum and plated in a 96-well plate (5×10^5 cells per well). Cells were incubated with directly conjugated antibodies for 30 minutes at 4°C. After washing, analysis was performed on a BD Accuri C6 flow cytometer. Antibodies used were FITC-anti-CD45 (1:200; eBiosciene); Alexa Flour 488-anti-CD184 (1:200; eBiosciene); and PE-anti-CD61 (1:200; eBioscience).

Platelet Isolation

Peripheral blood was collected from β3-floxed/Tie1Cre-negative/positive animals or from 15-day, OHT-treated β3-floxed/Pdgfb-iCreER^{T2}-negative/positive animals in tubes containing anticoagulant buffer (38 mmol/L citric acid, 75 mmol/L sodium citrate, 100 mmol/L dextrose). Blood samples were centrifuged for 10 minutes at 100*g*. The resulting platelet-rich plasma was transferred to a fresh tube and centrifuged for 10 minutes at 400*g*. The final pellet was lyzed in electrophoresis sample buffer and processed for Western blot analysis.

Flow Cytometry

LuECs were analyzed as described previously.[25] Antibodies used and detailed staining parameters can be found in the Online Data Supplement.

Western Blot Analysis

Western blot analysis was performed as described previously.[20] Antibodies used and detailed staining parameters can be found in the Online Data Supplement.

Adhesion Assays

These assays were performed as described previously.[10,26] Detailed parameters can be found in the Online Data Supplement.

Wound Closure Assay

In vitro scratch wound assays were performed as described previously.[12] Detailed parameters can be found in the Online Data Supplement.

Statistical Analysis

Significant differences between means were evaluated by Student *t* test. $P<0.05$ was considered statistically significant.

Results

Tumor Growth and Angiogenesis Are Inhibited in β3-Floxed/Pdgfb-iCreER^{T2} Animals, but Not in β3-Floxed/Tie1Cre Animals

To our surprise, the effects on tumor growth and angiogenesis in the 2 Cre models differed significantly from β3-knockout animals. Tie1Cre-mediated long-term depletion of endothelial β3-integrin did not significantly affect growth or angiogenesis of either B16F0 or CMT19T tumor cells (Figure 1A) after 12 days. Whereas, OHT-induced acute depletion of the protein via Pdgfb-iCreER^{T2} inhibited growth and angiogenesis in both tumor models (Figure 1B). On a detailed histological analysis of tumor sections, we observed no changes in tumor vessel pericyte or basement membrane coverage (Online Figure IA), or in overall vessel distribution across tumors (Online Figure IB), when drawing comparisons between Cre-negative and Cre-positive animals, or between the 2 Cre models. We also analyzed vessel perfusion in thick (vibratome) sections from CMT19T tumors (B16F0 tumors are too soft for vibratome sectioning). Vessel patency (as measured by intravenous injection of PE-labeled anti-PECAM1) was limited to a thin ring around the outer perimeter of the tumor (Online Figure IC) and was of a similar depth in β3-floxed/Tie1Cre-negative, β3-floxed/Tie1Cre-positive, and β3-floxed/Pdgfb-iCreER^{T2}-negative animals. Patent vessels penetrated deeper in β3-floxed/Pdgfb-iCreER^{T2}-positive tumors, but this could be attributed to their much smaller size (ie, these tumors have not yet established a poorly vascularized core). We then extended our analyses of the 2 Cre models by examining microvessel sprouting from aortic rings. VEGF-induced sprouting (measured on day 6) was significantly enhanced on Tie1Cre-mediated depletion of β3-integrin and inhibited on its Pdgfb-iCreER^{T2}-mediated depletion (Figure 1C).

One possible explanation for the difference between the 2 models is the nonendothelial-specific (leaky) expression of the 2 promoters used to drive Cre expression. The Pdgfb promoter can be expressed in megakaryocytes,[22] but we did not observe any changes in platelet levels of β3-integrin in either Cre line (Online Figure IIA). Furthermore, β3-floxed/P*f*4Cre (a platelet-specific Cre)[27] mice do not show any significant effects on tumor growth.[17] More importantly, Tie1 is expressed by a small proportion (≈20%) of BMD hematopoietic cell lineages[21] (as opposed to other constitutive endothelial-specific Cre models, such as Tie2Cre, which is reportedly expressed in ≈80%).[28] We examined β3-integrin expression in BMDCs from both Cre models. Although we saw no changes in β3-integrin in BMDCs of OHT-treated Pdgfb-iCreER^{T2}-positive animals, Tie1Cre-positive animals showed a loss of β3-integrin expression in CD45$^+$ cells (CD45 is a PAN marker for hematopoietic cells, including hematopoietic progenitor/stem cells but excluding erythrocytes and platelets; Online Figure IIB). Tie1Cre-positive animals did not, however, show loss of β3-integrin expression in CXCR4 (CD184)-expressing cells. The majority of BMDCs recruited to angiogenic sites express CXCR4, and the loss of β3-integrin expression in these cells would be expected to impinge on tumor angiogenesis.[29] We speculated that the absence of β3-integrin depletion in CXCR4$^+$ cells (primarily macrophages)[29] explains why, unlike β3-integrin–knockout mice, β3-floxed/Tie1Cre-positive mice do not exhibit enhanced tumor growth and angiogenesis in vivo. We examined this by performing flow cytometry on whole tumor homogenates from β3-floxed/Tie1Cre-positive and -negative animals. Our speculation was supported by the fact that we saw no changes in β3-integrin levels in F4/80-positive tumor-associated macrophages from β3-floxed/Tie1Cre-positive animals (Online Figure IIC).

Some Cellular and Molecular Differences Occur Between the 2 Cre Models

It is possible that phenotypic differences between the 2 Cre models are a result of variances in molecular compensation arising from either long- or short-term β3-integrin depletion. This prompted us to examine endothelial cell (EC) characteristics in greater detail. We isolated LuECs from β3-floxed/Tie1Cre animals and from β3-floxed/Pdgfb-iCreER^{T2} animals that were treated with OHT in vivo for 15 days before isolation and compared their biological and molecular characteristics in vitro. Although they showed an expected defect in adhesion to vitronectin, Cre-positive LuECs from both models showed adhesion to fibronectin, collagen type I, and laminin-I that was comparable to their Cre-negative counterparts (Online Figure IIIA). Using flow cytometric analysis (Figure 2A), we showed that surface expression of β3-integrin was depleted to similar levels in Cre-positive cells from both models. α1-, α5-, αv-, and β1-integrin subunit levels were similar in all cells, whereas α2-integrin levels seemed to decrease in Cre-positive cells from both models (note, however, that the levels of α1- and α2-integrin were particularly low in all cells). Although we were unable to detect surface expression of β5-integrin in our cultured ECs, Western blot analysis showed a decrease in total levels of this integrin subunit in β3-floxed/Tie1Cre-positive LuECs, but not in β3-floxed/Pdgfb-iCreER^{T2} LuECs (Figure 2A).

We saw no changes in overall LuEC survival in culture (not shown), so we next examined VEGF-induced migration, an essential feature of EC behavior that is mediated by integrins, by performing wound closure assays. Acute depletion of β3-integrin inhibited wound closure, whereas long-term depletion had no effect (Online Figure IIIB). Because we continued to observe some differences between the 2 Cre models, we decided to investigate in detail VEGF-mediated signaling. We first examined VEGFR2 expression and phosphorylation. Neither Cre model elicited changes in total levels of VEGFR2 expression (Figure 2B). However, acute depletion of β3-integrin led to a reduction in VEGF-induced VEGFR2 phosphorylation, whereas no changes were noted on long-term depletion of β3-integrin (Figure 2B). Another important function of αvβ3-integrin is the regulation of VEGFR2 recycling back to the cell surface,[30] so we examined surface expression of VEGFR2 by flow cytometry. We observed a small but significant increase

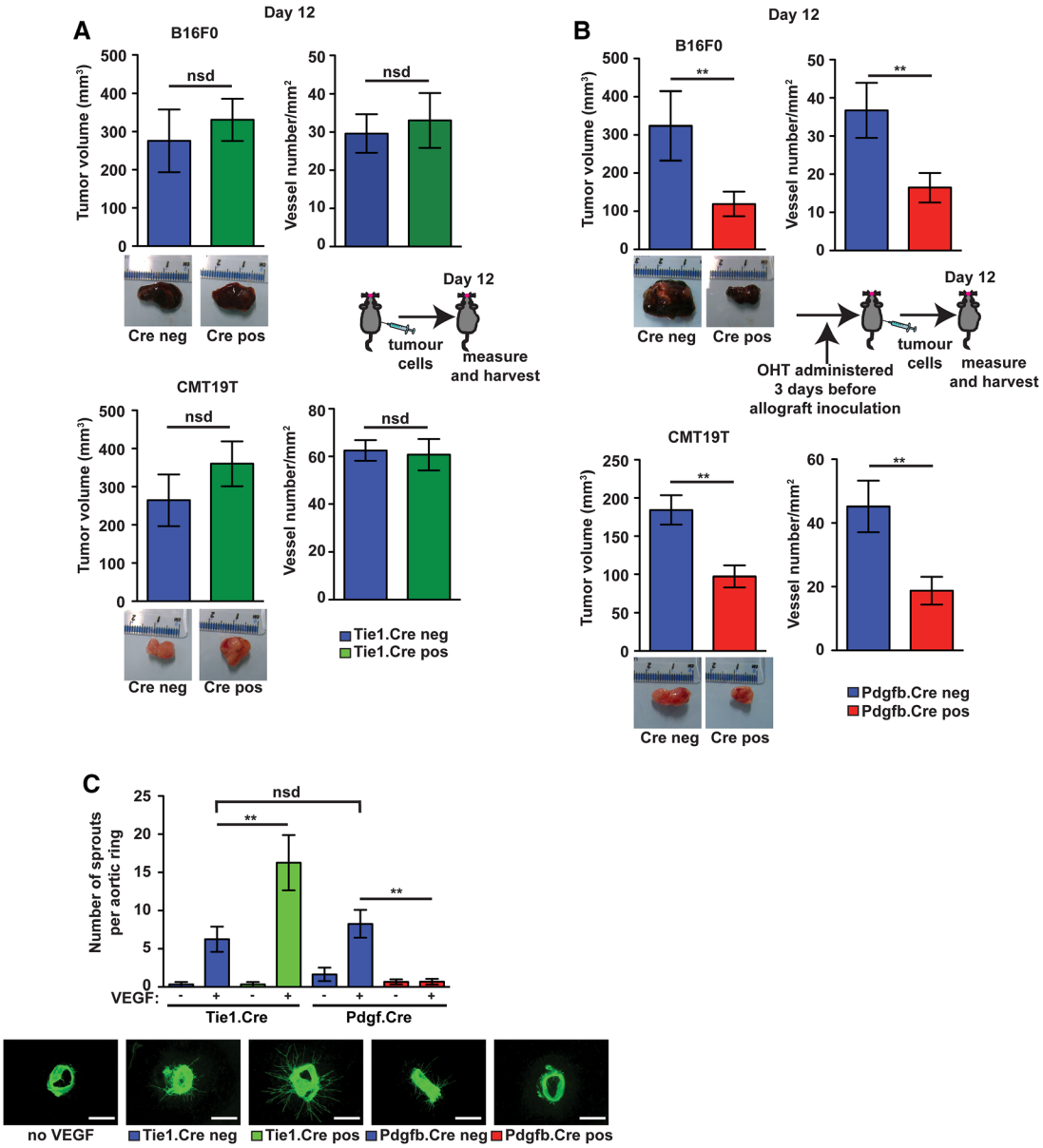

Figure 1. Acute, but not long-term, loss of β3-integrin reduces tumor growth and inhibits angiogenesis ex vivo, without altering tumor vessel structure or distribution. Tumor growth and angiogenesis were measured in (**A**) β3-floxed/Tie1Cre-negative (neg) and -positive (pos) littermates, and in (**B**) 4-hydroxy-tamoxifen (OHT)-treated β3-floxed/Pdgfb-iCreER^{T2}-neg and -pos littermates. Mice were given subcutaneous injections of B16F0 and CMT19T syngeneic tumor cell lines (see insets for schemes; **left**). Tumor volumes were measured 12 days later. Bar charts show mean tumor volumes (±SEM). Representative pictures of tumor macroscopic appearances are shown. Blood vessel density was assessed by counting the total number of endomucin-positive vessels across entire tumor sections (**right**). Bar charts show mean vessel numbers per mm^2 (±SEM). Data are representative of 3 independent experiments, where n≥5 mice per genotype per experiment. **C** (**top**), Microvessel sprouting of aortic ring explants isolated from β3-floxed/Tie1Cre and β3-floxed/Pdgfb-iCreER^{T2} mice was stimulated with vascular endothelial growth factor (VEGF). Unstimulated rings were used as a negative control. Rings from β3-floxed/Pdgfb-iCreER^{T2} mice were isolated from non-OHT–treated animals and were then cultured in the continued presence of 1 μmol/L OHT. Bar chart shows total number of microvessel sprouts per aortic ring (mean±SEM) after 6 days of VEGF stimulation. Data are representative of 3 experiments where n≥20 rings per genotype per experiment. Representative micrographs of FITC-IB4 (an endothelial cell marker)-stained aortic rings (**bottom**). Scale bar, 1 mm. Note that OHT treatment itself does not affect microvessel sprouting, as illustrated by similar VEGF-induced responses in TieCre-neg compared with Pdgfb-iCreER^{T2}-neg aortic rings. nsd indicates not significantly different; $^{**}P<0.01$ (unpaired 2-tailed *t* test). Note that in in vivo studies, β3-floxed/Pdgfb-iCreER^{T2} mice have been treated for a total of 15 days with OHT.

in surface expression of VEGFR2 in β3-floxed/Tie1Cre-positive LuECs compared with their Cre-negative controls (Figure 2C). This small increase was similar to that noted in β3-integrin–null LuECs when they are compared with wild-type LuECs (Figure 2C). No changes occurred in β3-floxed/Pdgfb-iCreER^{T2}-positive LuECs. To examine a wide spectrum of signaling pathways simultaneously, LuECs were stimulated with VEGF, and protein lysates were put onto PathScan Intracellular Signaling Arrays. The only signaling molecule to show any change between Cre-negative and Cre-positive

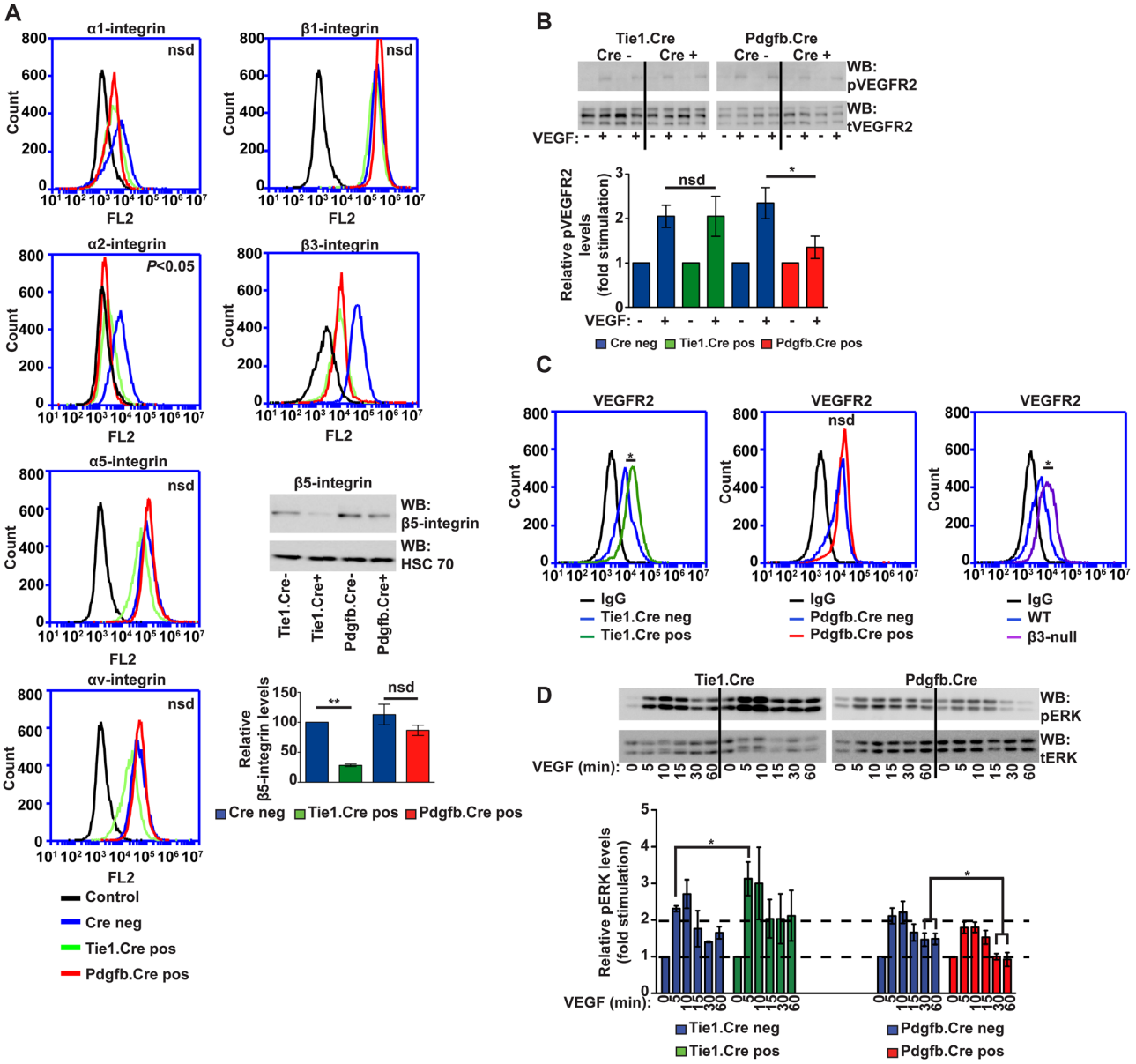

Figure 2. Characterization of endothelial cells isolated from Tie1Cre and Pdgfb-iCreER^{T2} lines. A, Representative flow cytometric profiles for α1-, α2-, α5-, αv-, β1-, and β3-integrin subunit expression levels on the indicated lung microvascular endothelial cells (LuECs). Isotype-matched profiles are shown as controls (black). β5-Integrin expression was analyzed by Western blot. HSC70 is shown as a loading control. Bar chart represents the mean (±SEM) densitometric quantification of total β5-integrin levels over multiple experiments (n≥3) shown relative to Tie1Cre-negative cells. **B**, Western blot analysis of vascular endothelial growth factor receptor 2 (VEGFR2) phosphorylation in LuECs. Cells were stimulated with 30 ng/mL VEGF for 5 minutes. Protein lysates were Western blotted for phosphorylated VEGFR2 (pVEGFR2; Y1175) and subsequently reblotted for total VEGFR2 (tVEGFR2). Data are representative of 3 independent experiments; 2 separate lysates are shown. Bar chart represents the mean (±SEM) densitometric quantification of pVEGFR2 levels relative to non-VEGF–treated cells (fold stimulation) over multiple experiments. **C**, Representative flow cytometric profiles of VEGFR2 expression levels on LuECs. IgG isotype control is shown as a control (black). **D**, Western blot analysis of ERK1/2 phosphorylation in LuECs. Cells were stimulated with 30 ng/mL VEGF for the indicated times. Protein lysates were Western blotted for phosphorylated ERK1/2 (pERK) and subsequently reblotted for total ERK1/2 (tERK). Data are representative of 4 independent experiments. Bar chart represents the mean (±SEM) densitometric quantification of pERK levels relative to non-VEGF–treated cells (fold stimulation) over multiple experiments. Values have been normalized to tERK levels. Hashed lines demarcate baseline and 2-fold stimulation levels.

animals (in both models) was ERK1/2 (not shown). We, therefore, examined VEGF-induced ERK1/2 phosphorylation in greater detail in cultured LuECs and showed that, compared with Cre-negative controls, ERK1/2 phosphorylation was enhanced in β3-floxed/Tie1Cre-positive LuECs, but suppressed in β3-floxed/Pdgfb-iCreER^{T2}-positive LuECs (Figure 2D). However, this kit did not include many important angiogenic signaling components, so we analyzed other VEGF-induced signaling molecules by Western blot analyses. Given our β5-integrin findings and the known link between αv-integrins and VEGF-dependent migration–associated molecules, such as Src and FAK,[31–33] we focused mainly on this pathway. We

observed a reduction in the levels of phosphorylated and total FAK in β3-floxed/Tie1Cre-positive LuECs (Online Figure IIIC). However, consistent with our PathScan findings, we saw no changes in p38 phosphorylation, which is also associated with this pathway. We, therefore, examined other players in the αv-integrin–FAK pathway, such as mTOR, S6 Ribosomal Protein (p70S6K), and PDK-1.[34] The PathScan array showed no changes in mTOR or p70S6K, nor did we observe any changes in PDK-1 phosphorylation by Western blot (Online Figure IIIC). Finally, we examined responses to fibroblast growth factor in both LuECs and aortic rings. We observed no differences in ERK1/2 phosphorylation (Online Figure IVA) nor in aortic ring sprouting (Online Figure IVB), suggesting that the responses described above are, at least partially, VEGF-specific.

Pattern of Cre Activity and Efficiency of β3-Integrin Depletion Are Similar in the 2 Endothelial Cre Models

Multiple other possibilities may explain the dichotomous effects we observed between the 2 Cre models. We examined each of these in turn and noted no significant differences when comparing: (1) VEGFR2 expression levels (Figure 3A–3C and as noted in Figure 2B). This was important to examine at multiple levels because a global deletion of β3-integrin can lead to the upregulation of endothelial VEGFR2 expression,[11] and changes in VEGFR2 expression levels might have explained differences in VEGF responses when comparing the 2 Cre models; (2) the efficiency of Cre-induced β3-integrin depletion. We showed this by both Western blot analyses (Figure 3A–3C) and in whole tumors (Figure 3D); (3) the pattern of Cre activity (as measured by tomato Cre reporter activity)[35] in the experimental models we used (Figure 3E and 3F). The Pdgfb promoter, in particular, may be highly active in endothelial tip cells, specialized cells found at the leading edge of angiogenic sprouts that are highly motile,[36] and differences in Cre activity between the 2 models in this population of cells (and hence differences in β3-integrin depletion) could explain differential effects on angiogenic responses.[37] However, we saw no differences in the distribution of Cre activity when comparing the 2 models in aortic rings; Cre was active in both tip and stalk cells in both Tie1Cre and Pdgfb-iCreER^{T2} rings (Figure 3F). Taking these findings in sum, we concluded that the length of time β3-integrin had been depleted was the major factor determining the angiogenic response and dictating the differences observed between our 2 endothelial Cre models.

Pdgfb-iCreER^{T2} Model Behaves Like the Tie1Cre Model if the Time of β3-Integrin Depletion Is Extended by Longer OHT Treatment

Given that the models differ in the amount of time that β3-integrin has been depleted, we extended the time of OHT treatment of Pdgfb-iCreER^{T2} animals before allograft administration to determine whether β3-floxed/Pdgfb-iCreER^{T2} mice would behave more like β3-floxed/Tie1Cre mice. We saw no effect on tumor growth or angiogenesis when tumor cell administration was preceded by 21 days of OHT treatment (for a total of 33 days of OHT treatment, henceforth referred to as long OHT). The inhibitory effects previously observed with acute depletion of endothelial β3-integrin (OHT administered 3 days before allograft administration, for a total of 15 days of treatment, henceforth referred to as short OHT) were completely abrogated (Figure 4A). A reciprocal loss of angiogenic inhibition was also observed in aortic rings derived from β3-floxed/Pdgfb-iCreER^{T2}-positive long OHT animals (Figure 4B). A side-by-side comparison of tumor growth in the 3 models illustrated similar growth kinetics of CMT19T tumor cells in β3-floxed/Tie1Cre and β3-floxed/Pdgfb-iCreER^{T2} long OHT mice; only in β3-floxed/Pdgfb-iCreER^{T2}-positive short OHT animals was tumor growth inhibited (Figure 4C). We conclude that by disrupting β3-integrin well before tumor induction, β3-floxed/Pdgfb-iCreER^{T2} animals behave like β3-floxed/Tie1Cre animals, and more importantly, there is a complete loss of preventive benefit with long-term depletion of endothelial β3-integrin.

Further Characterization of Angiogenesis in β3-Floxed/Pdgfb-iCreER^{T2} Long OHT Animals Uncovers Commonalities With β3-Floxed/Tie1Cre Animals

We next examined many of the parameters noted above in LuECs isolated from β3-floxed/Pdgfb-iCreER^{T2} mice treated for 33 days in vivo with OHT. When comparing β3-floxed/Pdgfb-iCreER^{T2}-positive long OHT LuECs with their Cre-negative counterparts, we noted similar changes to those observed in β3-floxed/Tie1Cre-positive LuECs: (1) only defects in adhesion to vitronectin (Online Figure VA); (2) no change in VEGF-induced wound closure (Online Figure VB); (3) unaltered levels of integrin subunit surface expression, but a reduction in total levels of β5-integrin expression (Figure 5A); (4) no changes in VEGF-mediated VEGFR2 phosphorylation, but an increase in expression of VEGFR2 at the cell surface (Figure 5B); and (5) no alterations in VEGF-induced ERK1/2 phosphorylation (Figure 5C). Additionally, we examined pericyte and basement coverage of tumor vessels, as well as vessel distribution and patency and noticed no overt differences between long OHT Cre-negative and Cre-positive animals (Online Figure VI). We speculate that long-term depletion of β3-integrin, regardless of the Cre driving the depletion, leads to common mechanisms of escape from the otherwise inhibitory effects of interfering with the endothelial expression of this molecule.

We recently showed that a 50% reduction in FAK expression in FAK-heterozygous mice leads to enhanced tumor growth and angiogenesis.[23] FAK-heterozygous ECs display an imbalance in FAK phosphorylation at Y397 and Y861, which suggests a potential role for FAK as a nonlinear, dose-dependent regulator of angiogenesis. Therefore, we next examined changes in FAK expression and phosphorylation in our β3-floxed/Cre models in greater detail. Western blot analysis indicated that total FAK levels were reduced by ≈50% in β3-floxed/Tie1Cre-positive and β3-floxed/Pdgfb-iCreER^{T2}-positive long OHT LuECs, but not in β3-floxed/Pdgfb-iCreER^{T2}-positive short OHT LuECs, as were levels of phosphorylation of FAK at Y397. Levels of phosphorylation of FAK at Y861, however, were similar in all LuECs (Figure 6A; Online Figure VII). We extended these studies to examine FAK expression in tumor blood vessels. Histological analysis revealed reduced levels of FAK expression in tumor vasculature of β3-floxed/Tie1Cre-positive animals

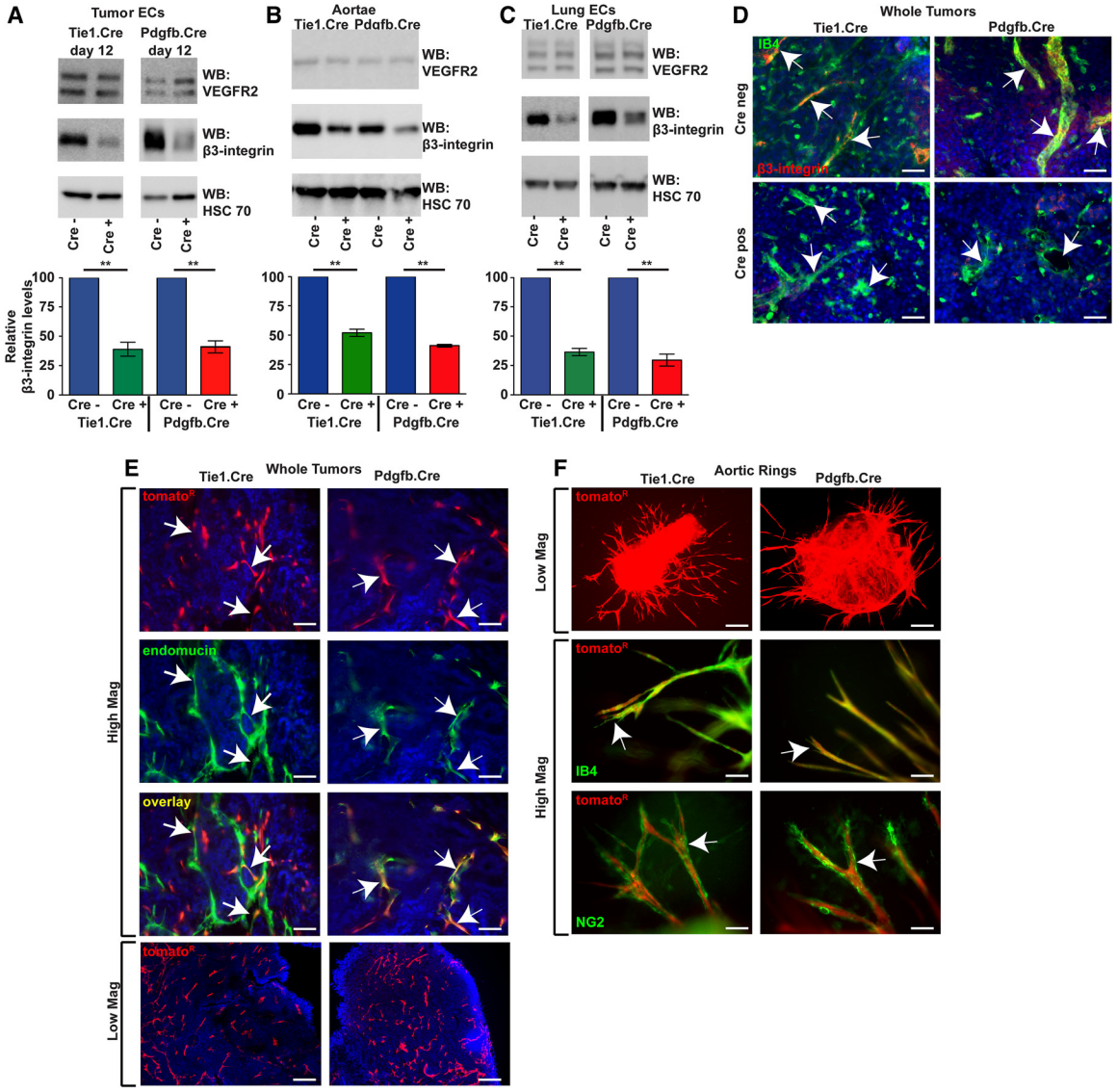

Figure 3. Further characterization of Tie1Cre and Pdgfb-iCreER^{T2} models. A, Analyses of protein expression in isolated tumor endothelial cells. Representative Western blot analysis (**top**) of vascular endothelial growth factor receptor 2 (VEGFR2) and β3-integrin expression in tumor endothelial cells (ECs) isolated from 12-day allografts grown in β3-floxed/Tie1Cre mice and 4-hydroxy-tamoxifen (OHT)-treated β3-floxed/Pdgfb-iCreER^{T2} mice. HSC70 serves as a loading control. Bar chart (**bottom**) represents the mean (±SEM) densitometric quantification of relative β3-integrin levels measured over 3 separate experiments. **B**, Analyses of protein expression in whole aortae. Representative Western blot analysis (**top**) of VEGFR2 and β3-integrin expression in aortae isolated from β3-floxed/Tie1Cre mice and OHT-treated (15 days) β3-floxed/Pdgfb-iCreER^{T2} mice. HSC70 serves as a loading control. Bar chart (**bottom**) represents the mean (±SEM) densitometric quantification of relative β3-integrin levels measured over 3 separate experiments. **C**, Analyses of protein expression in isolated lung microvascular endothelial cells (ECs). Representative Western blot analysis (**top**) of VEGFR2 and β3-integrin expression in lung ECs isolated from β3-floxed/Tie1Cre-negative and -positive mice and 15-day, OHT-treated β3-floxed/Pdgfb-iCreER^{T2}-negative and -positive mice. HSC70 serves as a loading control. Bar chart (**bottom**) represents the mean densitometric quantification of relative β3-integrin levels measured over 3 individual isolates of each genotype (±SEM). $^{**}P<0.01$ (unpaired 2-tailed *t* test). **D**, Analyses of protein expression in whole tumor sections. Representative immunofluorescence analysis of peripheral blood vessels (arrows) costained with FITC-IB4 lectin (an endothelial cell marker; green) and lumenal β3-integrin, which was detected by intravenous injection of a directly conjugated antibody (red). Scale bar, 50 μm. **E**, Analysis of Cre expression pattern in whole tumor sections. Representative high-magnification immunofluorescence analysis (**top**, 3 panels) showing that tomato Cre reporter activity (tomato^R; red) overlaps with blood vessels (arrows) that have been costained with endomucin (an endothelial cell marker; green) in tumors grown in either Tie1Cre-positive or OHT-treated Pdgfb-iCreER^{T2}-positive mice. The 3 arrows point to identical locations in each micrograph. Scale bar, 50 μm. Representative low-magnification immunofluorescence analysis (**bottom**) showing widespread tomato Cre reporter activity (tomato^R; red) in tumors grown in Tie1Cre-positive or OHT-treated Pdgfb-iCreER^{T2}-positive mice. Scale bar, 400 μm. **F**, Representative low-magnification immunofluorescence analysis showing that both Tie1Cre- and OHT-treated Pdgfb-iCreER^{T2} aortic rings exhibit tomato Cre reporter activity (tomato^R; red) in all microvascular sprouts after 6 days of VEGF stimulation (**top**). Scale bar, 0.5 mm. Representative high-magnification immunofluorescence analysis showing tomato Cre reporter activity (tomato^R; red) overlapping with endothelial cells that have been costained with FITC-IB4 lectin (green) in both Tie1Cre- and OHT-treated Pdgfb-iCreER^{T2} aortic rings (**middle**). Arrows point to tip cells (with their filipodia extensions). Scale bar, 50 μm. Representative high-magnification immunofluorescence analysis showing that tomato Cre reporter activity (tomato^R; red) does not overlap with pericytes that have been costained with anti-NG2 (green) in either Tie1Cre- or OHT-treated Pdgfb-iCreER^{T}2 aortic rings (**bottom**). Arrows point to pericyte cells. Scale bar, 50 μm.

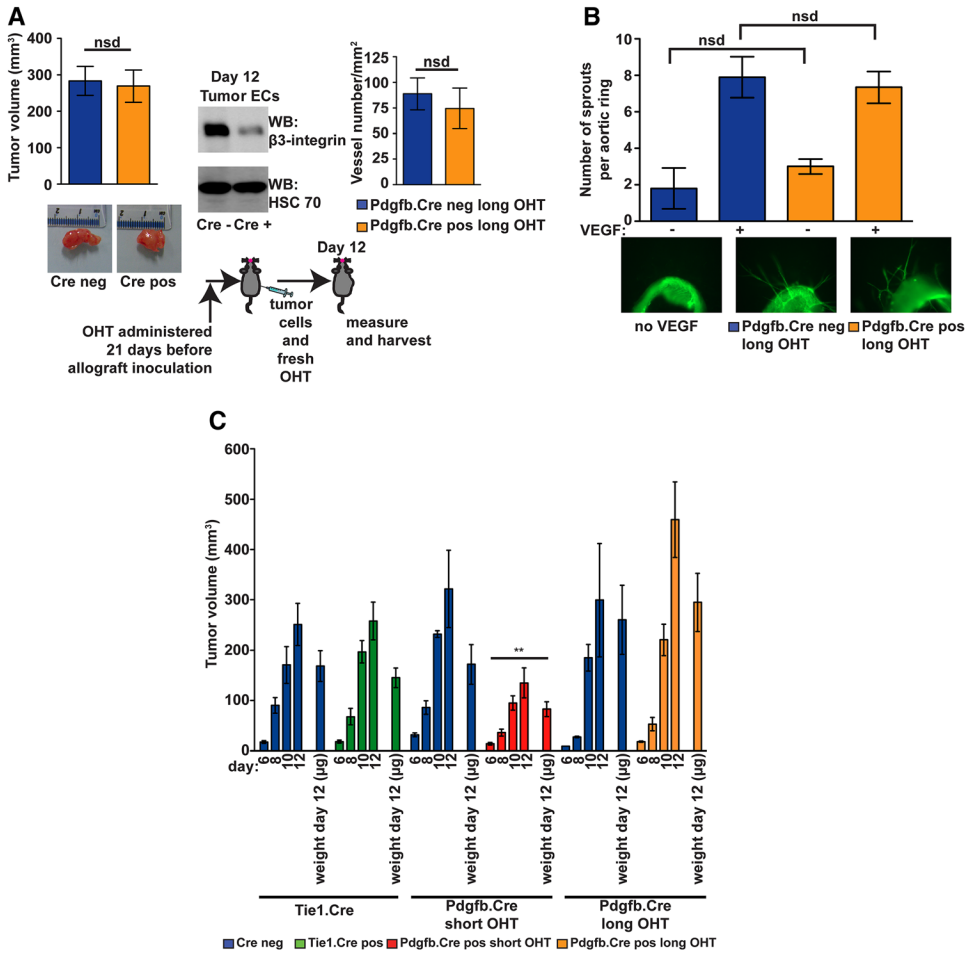

Figure 4. Timing of endothelial β3-integrin depletion determines the angiogenic response. A, Analysis of CMT19T tumor growth in β3-floxed/Pdgfb-iCreER^{T2} animals that were pretreated with 4-hydroxy-tamoxifen (OHT) for 21 days before allograft administration (see inset for scheme). Fresh OHT treatment was started at the time of allograft injection (for a total of 33 days of OHT treatment; long OHT). Twelve-day-old tumor volumes showed no statistical difference between Cre-negative and Cre-positive littermates (**left**). Bar chart shows mean tumor volume (±SEM). Representative pictures of tumor macroscopic appearances are shown. Representative Western blot analysis of endothelial cells (ECs) isolated from CMT19T tumors grown in long OHT–treated β3-floxed/Pdgfb-iCreER^{T2} mice (**middle**). HSC70 acts as a loading control. Blood vessel density was assessed by counting the total number of endomucin-positive vessels per mm^2 across entire tumor sections (**right**). Bar chart shows mean vessel number per mm^2 (±SEM). Data are representative of 3 independent experiments, where n=5 mice per genotype per experiment. **B**, Microvessel sprouting of aortic ring explants isolated from long OHT–treated β3-floxed/Pdgfb-iCreER^{T2} mice was stimulated with vascular endothelial growth factor (VEGF). Unstimulated rings were used as a negative control. Bar chart shows total number of microvessel sprouts per aortic ring (mean±SEM) after 6 days of VEGF stimulation (in the continued presence of 1 μmol/L OHT). Data are representative of 3 experiments where n≥20 rings per genotype per experiment. Representative micrographs of FITC-IB4 (an endothelial cell marker)-stained aortic rings (**bottom**). Scale bar, 0.5 mm. **C**, Direct comparison of CMT19T tumor growth in the 3 models. Tumor cells were injected subcutaneously in β3-floxed/TieCre mice, β3-floxed/Pdgfb-iCreER^{T2} mice pretreated for 3 days with OHT (for a total of 15 days; short OHT), and β3-floxed/Pdgfb-iCreER^{T2} mice pretreated for 21 days with OHT (for a total of 33 days; long OHT). Bar chart shows mean tumor volume (±SEM) as measured externally by calipers over time. Also shown is the mean tumor weight in micrograms (±SEM) at the end of the experiment. n≥5 animals per genotype; $^{**}P<0.01$; nsd, no significant difference (unpaired 2-tailed *t* test).

and β3-floxed/Pdgfb-iCreER^{T2}-positive long OHT animals, but not in β3-floxed/Pdgfb-iCreER^{T2}-positive short OHT animals (Figure 6B). These findings suggest that prolonged suppression of endothelial β3-integrin leads to a reduction in FAK expression and a misbalance in FAK phosphorylation that helps circumvent the inhibitory effects mediated by the loss of β3-integrin.

Tumor Growth and Angiogenesis Are Not Inhibited by β3-Integrin Depletion in Already Established Tumors

Finally, we extended our analyses with the Pdgfb-iCreER^{T2} (short OHT) line to more clinically relevant models of tumor growth. Prolonging the growth of CMT19T allografts by an additional 6 days (still within their exponential growth phase) in Pdgfb-iCreER^{T2}– depleted mice negated the inhibitory effects observed at day 12 (Figure 7A). We could not extend treatment of B16F0 allografts, because these tumors grow extremely rapidly beyond day 12 and reach a plateau phase of growth by day 13 or 14.

To test the effects of β3-integrin disruption in tumors with established vasculature, we used an intervention treatment scheme. This scheme mimics the common clinical situation of treating patients with established tumors and evaluating effects on tumor progression. B16F0 or CMT19T tumor cells were implanted subcutaneously and OHT was administered

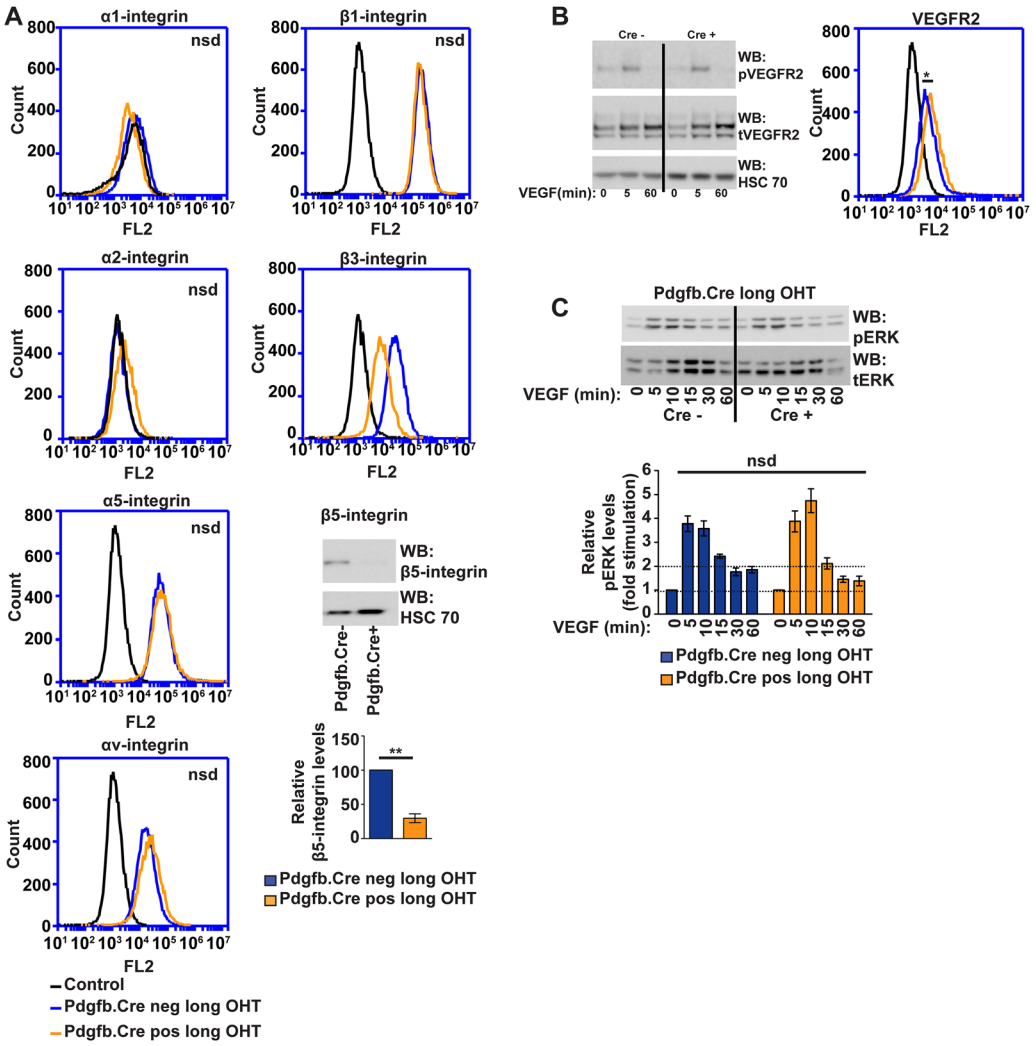

Figure 5. Further characterization of the long 4-hydroxy-tamoxifen (OHT)-treated Pdgfb-iCreER^{T2} lung endothelial cells. A, Representative flow cytometric profiles for α1-, α2-, α5-, αv-, β1-, and β3-integrin subunit expression levels on long OHT–treated lung microvascular endothelial cells (LuECs). Isotype-matched profiles are shown as controls (black). β5-Integrin expression was analyzed by Western blot. HSC70 is shown as a loading control. Bar chart represents the mean (±SEM) densitometric quantification of total β5-integrin levels over multiple experiments (n≥3) shown relative to Cre-negative cells. **B**, Western blot analysis of vascular endothelial growth factor receptor 2 (VEGFR2) phosphorylation in long OHT–treated LuECs (**left**). Cells were stimulated with 30 ng/mL of VEGF for 5 or 60 minutes. Protein lysates were Western blotted for phosphorylated VEGFR2 (pVEGFR2; Y1175) and subsequently reblotted for total VEGFR2 (tVEGFR2). Data are representative of 3 independent experiments. Representative flow cytometric profile of VEGFR2 expression levels on long OHT–treated LuECs. IgG isotype control is shown as a control (black; **right**). **C**, Western blot analysis of ERK1/2 phosphorylation in long OHT–treated LuECs. Cells were stimulated with 30 ng/mL VEGF for the indicated times. Protein lysates were Western blotted for phosphorylated ERK1/2 (pERK) and subsequently reblotted for total ERK1/2 (tERK). Data are representative of 3 independent experiments. Bar chart represents the mean (±SEM) densitometric quantification of pERK levels relative to non-VEGF–treated cells (fold stimulation) over multiple experiments. Values have been normalized to tERK levels. Hashed lines demarcate baseline and 2-fold stimulation levels. *P<0.05; **P<0.01; nsd, no significant difference (unpaired 2-tailed t test). Note that no OHT was present during the culturing of cells; β3-integrin depletion was induced before isolation.

after 8 days. Tumor volumes were assessed 5 and 10 days later. Although substantial β3-integrin depletion was achieved in TECs, no significant differences were observed between β3-floxed/Pdgfb-iCreER^{T2}-negative and -positive animals at day 13 (B16F0 tumors had to be harvested at this stage for the reasons described above; see Online Figure VIII) or day 18 (Figure 7B). We also used an intervention strategy in the aortic ring neoangiogenesis assay by inducing β3-integrin depletion in aortic rings derived from β3-floxed/Pdgfb-iCreER^{T2} animals after microvessel sprouting had already begun (3 days after their embedding and VEGF stimulation). Sprouts were then counted at day 8. Cre activity was established <24 hours (as measured by tomato Cre reporter activity), yet no significant differences were observed in the degree of sprouting when comparing Cre-negative aortic rings with Cre-positive aortic rings (Figure 7C).

Discussion

β3-Integrin–knockout mice exhibit a complex phenotype that includes enhanced pathological angiogenesis. However, as mentioned above, β3-integrin is expressed by a diverse set of cells, and the described phenotype must arise from the integration of its pattern of expression. Although interesting, this

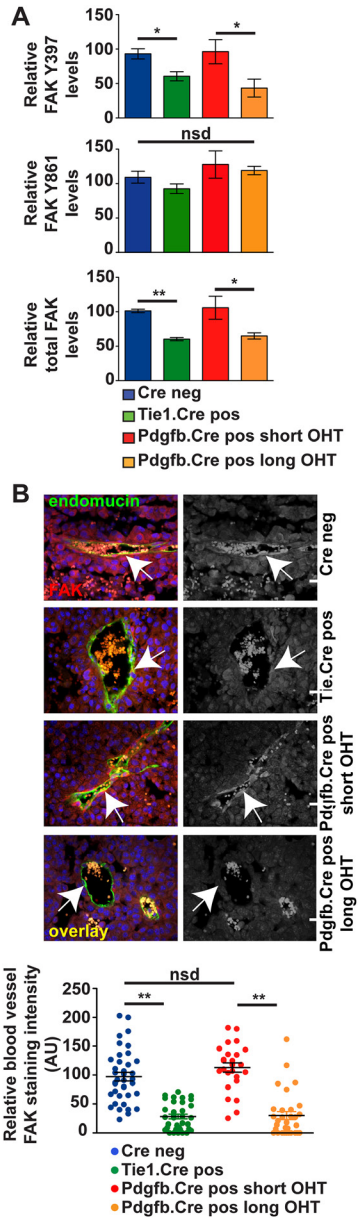

Figure 6. Reduced focal adhesion kinase (FAK) expression in β3-floxed/Tie1Cre and long 4-hydroxy-tamoxifen (OHT)-treated β3-floxed/Pdgfb-iCreER^{T2} animals. A, Analysis of FAK expression in lung endothelial cells. Bar charts represent the mean (±SEM) densitometric quantification of protein levels over multiple experiments (n>3) for phosphorylated FAKY397, phosphorylated FAKY861, and total FAK. **B**, Representative micrographs of immunofluorescence staining for FAK (red) and endomucin (green) in tumor sections from the indicated genotypes (**top**). Arrows point to examples of endothelial FAK staining. FAK-only staining is shown in grey scale micrographs. Scatter plot chart shows the mean fluorescent intensity (±SEM) of FAK levels per blood vessel (**bottom**). Data represent 3 tumors per genotype, ≥5 sections per tumor. Scale bars, 50 μm. *P<0.05; **P<0.01; nsd, no significant difference (unpaired 2-tailed t test).

biological integration makes it difficult to distinguish cell autonomous effects of β3-integrin. Our studies have addressed, for the first time to our knowledge, the specific contribution that endothelial β3-integrin makes to tumor growth and angiogenesis. Our findings have profound implications for targeting the endothelial-specific expression of β3-integrin to inhibit tumor angiogenesis, a strategy that is growing in popularity with the maturation of nanotechnology.[38]

Consistent with our findings in β3-knockout animals,[10] the depletion of endothelial β3-integrin did not alter the structure of established tumor vessels (Online Figure IA and Online Figure VIA). Sprouting angiogenesis involves an initial increase in EC proliferation, migration, and tube formation, followed by maturation of vessels that includes the recruitment of supporting cells and the deposition of an intact basement. Because we show deposition of a nidogen-rich basement membrane and the number of tumor vessels with associated αSMA-positive supporting cells is normal when endothelial β3-integrin is depleted (in both Cre models), we interpret our data to indicate that β3-integrin supports the initial phases of neovascularization. This conclusion is buttressed by 2 key findings: (1) genetic inhibition of endothelial β3-integrin is ineffective in an intervention strategy (once angiogenesis is in full swing, β3-integrin is not required; Figure 7B and 7C); (2) acute depletion of β3-integrin inhibited LuEC migration (athough not, notably, cell survival; Online Figure IIIB).

The αvβ3-integrin antagonist studies, which show the potential to inhibit angiogenesis both in vitro[39] and in vivo[16,40–42] when targeting the molecule, have always stood in seeming contrast to the enhanced angiogenesis observed in β3-integrin–knockout mice. The findings we present here help to marry the conflicting results and, more importantly, to explain further the disappointing clinical outcomes achieved to date with αvβ3-integrin antagonism. Our studies indicate that the timing of endothelial β3-integrin targeting is critical. As mentioned above, β3-integrin depletion does not inhibit tumor growth or angiogenesis when applied in an intervention type scheme (Figure 7B and 7C). Furthermore, early preventive benefit of β3-integrin depletion (which likely results from decreased interactions between αvβ3-integrin and VEGR2, leading to reduced VEGFR2 phosphorylation; Figure 2B) is lost over time (Figure 7A), an effect that is most pronounced with long-term depletion of the molecule, as demonstrated by β3-floxed/Tie1Cre animals and long OHT-treated β3-floxed/Pdgfb-iCreER^{T2} animals. By performing a detailed comparison, we have identified common changes that occur within the ECs of these 2 models: (1) increased surface expression of VEGFR2; (2) decreased total expression of β5-integrin; and (3) decreased expression (and misbalanced phosphorylation) of FAK. At least 1 of these alterations mimics what occurs in β3-knockout cells (altered surface expression of VEGFR2; Figure 2C). However, unlike the β3-integrin–knockout studies, long-term depletion of endothelial β3-integrin does not result in enhanced pathological angiogenesis in vivo, thus emphasizing that the increased tumor growth that occurs in β3-integrin–knockout mice is primarily a result of β3-integrin deletion in nonendothelial cells.[14,15,29] Tumor-associated macrophages seem to be unaltered in their levels of β3-integrin expression in β3-floxed/Tie1Cre-positive animals.

Any one of the changes we have identified might contribute to an escape from angiogenic inhibition directed at β3-integrin (in fact, it may be a sum of these and other changes that contribute to escape). For example, canstatin, an endogenous inhibitor of angiogenesis derived from the α2 chain of type IV collagen, binds αvβ5-integrin leading to activation in ECs of an apoptotic program.[43] With reduced levels of this integrin, a natural pathway that keeps

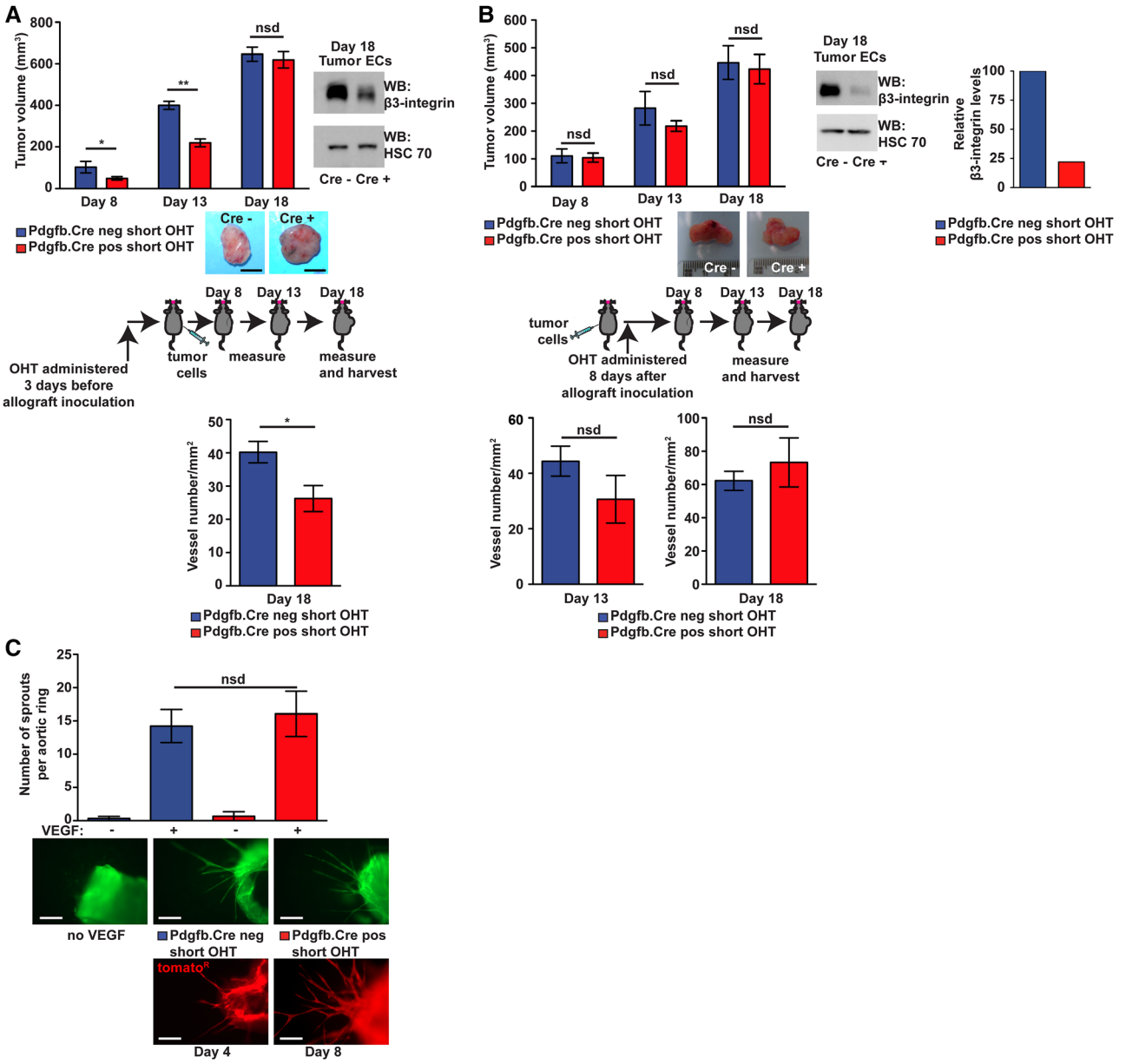

Figure 7. Effect of acute endothelial β3-integrin depletion is lost with time and is not effective if tumor growth and angiogenesis have already been established. A, Tumor growth was extended in short 4-hydroxy-tamoxifen (OHT)-treated β3-floxed/Pdgfb-iCreER^{T2} mice. Mice were given subcutaneous CMT19T tumor cells and volumes were measured via calipers at days 8, 13, and 18 (see insets for scheme; **top**). Bar chart shows mean tumor volumes (±SEM). Representative pictures of tumor macroscopic appearances at day 18 are shown. Scale bar, 1 cm. To the right is shown a representative Western blot analysis of β3-integrin levels in tumor endothelial cells isolated at day 18. HSC70 is shown as a loading control. Blood vessel density in 18-day tumors was assessed by counting the total number of endomucin-positive vessels per mm^2 across entire tumor sections (**bottom**). Bar chart shows mean vessel number per mm^2 (±SEM). Data are representative of 3 independent experiments, where n=5 mice per genotype per experiment. **B**, Tumor growth was initiated before OHT treatment. Mice were injected subcutaneously with CMT19T cells and OHT was administered 8 days later (**top**). Tumor volumes were measured via calipers at days 8, 13, and 18 (see insets for scheme). Bar chart shows mean tumor volumes (±SEM). Representative pictures of tumor macroscopic appearances at day 18 are shown. To the right is shown a representative Western blot analysis of β3-integrin levels in tumor endothelial cells isolated at day 18. HSC70 is shown as a loading control. Blood vessel density in 13-day and 18-day tumors (**bottom**) was assessed by counting the total number of endomucin-positive vessels per mm^2 across entire tumor sections. Bar chart shows mean vessel number per mm^2 (±SEM). Data are representative of 3 independent experiments, where n=5 mice per genotype per experiment. **C**, Microvessel sprouting of aortic ring explants isolated from non-OHT–treated β3-floxed/Pdgfb-iCreER^{T2} mice was stimulated with vascular endothelial growth factor (VEGF) 3 days before the addition of 1 μmol/L OHT (**top**). Bar chart shows total number of microvessel sprouts per aortic ring (mean±SEM) after 8 days of VEGF stimulation. Data are representative of 3 experiments where n≥20 rings per genotype per experiment. Representative micrographs of FITC-IB4–stained aortic rings (**middle**). Scale bar, 0.5 mm. Representative immunofluorescence analysis (**bottom**) showing tomato Cre reporter activity (tomato^R; red) in Pdgfb-iCreER^{T2}-positive aortic rings 24 hours (day 4) and 96 hours (day 8) after OHT administration (which was initiated on day 3). Scale bar, 0.5 mm. *P<0.05; nsd, no significant difference (unpaired 2-tailed t test).

angiogenesis in check has been removed. We chose to pursue the FAK findings in greater detail because of our recent publication of the FAK-heterozygous phenotype. However, there are differences. Unlike what we observed in the FAK-heterozygous studies, here we see no changes in Akt phosphorylation, which has been linked to the phenotype in FAK-heterozygous animals.[23] This suggests that the changes in Akt in FAK-heterozygous mice arise through a non-EC-autonomous route. No doubt, there are other changes occurring in our Cre models that have yet to be identified, which will help explain, for example, why Tie1Cre-mediated depletion of β3-integrin enhances angiogenic responses ex vivo, whereas long OHT-treated Pdgfb-iCreER^{T2}-mediated depletion does not.

Importantly, our findings parallel disappointing clinical studies showing similar results with long-term pharmacological inhibition of αvβ3-integrin.[16,44] In a recent phase III trial, Cilengitide (an RGD peptide antagonist of αvβ3-integrin and, to a lesser degree, of αvβ5-integrin) did not meet its primary end point of significantly increasing overall survival when added to the current standard chemoradiotherapy regimen.[45] This outcome suggests that we do not yet have the necessary knowledge or understanding of how best to use this promising antiangiogenic agent. We have shown previously that the dose of αvβ3-integrin antagonist achieved in vivo is important in the regulation of angiogenesis, a finding that illustrated the need to gain a more thorough understanding of how different doses of αvβ3-integrin–directed agents regulate angiogenesis.[25] Here, we show that the length of time endothelial αvβ3-integrin is inhibited may also be critical to angiogenic responses.

The studies we present here suggest that current αvβ3-integrin–directed strategies need refinement. This is a goal worth pursuing. Unlike current Food and Drug Administration–approved antiangiogenic drugs, αvβ3-integrin antagonists seem to be well tolerated,[46] likely because of the fact that the vascular expression of αvβ3-integrin is restricted to neoangiogenic vessels. In contrast, the targets of other antiangiogenic drugs are expressed in nearly all adult vascular endothelial cells,[47] and these drugs (especially those with broadspectrum activity) are linked with significant side effects, such as renal toxicity, bleeding, arterial thromboembolic events, wound healing complications, and gastrointestinal perforation, as well as vessel regression in several healthy tissues. Our next aim, then (using the models we have created), is to determine how mechanisms of escape that occur with endothelial β3-integrin inhibition can be circumvented, and to determine how these mechanisms can be targeted safely and effectively in combination with new or existing αvβ3-integrin antagonists to improve therapeutic outcomes.

Acknowledgments

We thank Samuel Atkinson who helped with some of the experiments during a British Society for Cell Biology-funded Summer Studentship in the laboratory. A special thanks to Ulrike Mayer for her wonderful mentoring of Stephen D. Robinson during the early stages of his independent career. V.S. designed and performed experiments, analyzed data, and helped edit the article. T.S.E. performed in vitro experiments, analyzed data, and helped edit the article. A.M.G. performed experiments and analyzed data. K.W. provided β3-floxed mice and helped edit the article. D.E. analyzed data and helped edit the article. J.G.S. generated β3-floxed mice and helped edit the article. M.F. provided Pdgfb-iCreER^{T2} mice. K.M.H.-D. provided initial support for the project and helped edit the article. S.D.R. designed experiments, performed experiments, analyzed data, and wrote the article.

Sources of Funding

V.S. was supported by a University of East Anglia dean's PhD studentship. T.S.E. was supported by a BigC PhD studentship. The work has also been supported by a start-up grant to S.D.R. from University of East Anglia School of Biological Sciences.

Disclosures

None.

References

1. Nussenbaum F, Herman IM. Tumor angiogenesis: insights and innovations. *J Oncol*. 2010;2010:132641.
2. Ruoslahti E, Pierschbacher MD. New perspectives in cell adhesion: RGD and integrins. *Science*. 1987;238:491–497.
3. Brooks PC, Clark RA, Cheresh DA. Requirement of vascular integrin alpha v beta 3 for angiogenesis. *Science*. 1994;264:569–571.
4. Brooks PC, Montgomery AM, Rosenfeld M, Reisfeld RA, Hu T, Klier G, Cheresh DA. Integrin alpha v beta 3 antagonists promote tumor regression by inducing apoptosis of angiogenic blood vessels. *Cell*. 1994;79:1157–1164.
5. Van Waes C. Cell adhesion and regulatory molecules involved in tumor formation, hemostasis, and wound healing. *Head Neck*. 1995;17:140–147.
6. Mahabeleshwar GH, Feng W, Reddy K, Plow EF, Byzova TV. Mechanisms of integrin-vascular endothelial growth factor receptor cross-activation in angiogenesis. *Circ Res*. 2007;101:570–580.
7. Brooks PC, Strömblad S, Klemke R, Visscher D, Sarkar FH, Cheresh DA. Antiintegrin alpha v beta 3 blocks human breast cancer growth and angiogenesis in human skin. *J Clin Invest*. 1995;96:1815–1822.
8. Srivatsa SS, Fitzpatrick LA, Tsao PW, Reilly TM, Holmes DR Jr, Schwartz RS, Mousa SA. Selective alpha v beta 3 integrin blockade potently limits neointimal hyperplasia and lumen stenosis following deep coronary arterial stent injury: evidence for the functional importance of integrin alpha v beta 3 and osteopontin expression during neointima formation. *Cardiovasc Res*. 1997;36:408–428.
9. Mahabeleshwar GH, Feng W, Phillips DR, Byzova TV. Integrin signaling is critical for pathological angiogenesis. *J Exp Med*. 2006;203:2495–2507.
10. Reynolds LE, Wyder L, Lively JC, Taverna D, Robinson SD, Huang X, Sheppard D, Hynes RO, Hodivala-Dilke KM. Enhanced pathological angiogenesis in mice lacking beta3 integrin or beta3 and beta5 integrins. *Nat Med*. 2002;8:27–34.
11. Reynolds AR, Reynolds LE, Nagel TE, Lively JC, Robinson SD, Hicklin DJ, Bodary SC, Hodivala-Dilke KM. Elevated Flk1 (vascular endothelial growth factor receptor 2) signaling mediates enhanced angiogenesis in beta3-integrin-deficient mice. *Cancer Res*. 2004;64:8643–8650.
12. Robinson SD, Reynolds LE, Kostourou V, Reynolds AR, da Silva RG, Tavora B, Baker M, Marshall JF, Hodivala-Dilke KM. Alphav beta3 integrin limits the contribution of neuropilin-1 to vascular endothelial growth factor-induced angiogenesis. *J Biol Chem*. 2009;284:33966–33981.
13. Robinson SD, Hodivala-Dilke KM. The role of beta3-integrins in tumor angiogenesis: Context is everything. *Curr Opin Cell Biol*. 2011;23:630–637.
14. Taverna D, Moher H, Crowley D, Borsig L, Varki A, Hynes RO. Increased primary tumor growth in mice null for beta3- or beta3/beta5-integrins or selectins. *Proc Natl Acad Sci U S A*. 2004;101:763–768.
15. Watson AR, Pitchford SC, Reynolds LE, Direkze N, Brittan M, Alison MR, Rankin S, Wright NA, Hodivala-Dilke KM. Deficiency of bone marrow beta3-integrin enhances non-functional neovascularization. *J Pathol*. 2010;220:435–445.
16. Stupp R, Ruegg C. Integrin inhibitors reaching the clinic. *J Clin Oncol*. 2007;25:1637–1638.
17. Morgan EA, Schneider JG, Baroni TE, Uluçkan O, Heller E, Hurchla MA, Deng H, Floyd D, Berdy A, Prior JL, Piwnica-Worms D, Teitelbaum SL, Ross FP, Weilbaecher KN. Dissection of platelet and myeloid cell defects by conditional targeting of the beta3-integrin subunit. *FASEB J*. 2010;24:1117–1127.
18. Germain M, De Arcangelis A, Robinson SD, Baker M, Tavora B, D'Amico G, Silva R, Kostourou V, Reynolds LE, Watson A, Jones JL, Georges-Labouesse E, Hodivala-Dilke K. Genetic ablation of the alpha 6-integrin subunit in Tie1Cre mice enhances tumour angiogenesis. *J Pathol*. 2010;220:370–381.
19. da Silva RG, Tavora B, Robinson SD, et al. Endothelial alpha3beta1-integrin represses pathological angiogenesis and sustains endothelial-VEGF. *Am J Pathol*. 2010;177:1534–1548.
20. Tavora B, Batista S, Reynolds LE, Jadeja S, Robinson S, Kostourou V, Hart I, Fruttiger M, Parsons M, Hodivala-Dilke KM. Endothelial FAK is required for tumour angiogenesis. *EMBO Mol Med*. 2010;2:516–528.

21. Gustafsson E, Brakebusch C, Hietanen K, Fässler R. Tie-1-directed expression of Cre recombinase in endothelial cells of embryoid bodies and transgenic mice. *J Cell Sci*. 2001;114:671–676.
22. Claxton S, Kostourou V, Jadeja S, Chambon P, Hodivala-Dilke K, Fruttiger M. Efficient, inducible Cre-recombinase activation in vascular endothelium. *Genesis*. 2008;46:74–80.
23. Kostourou V, Lechertier T, Reynolds LE, Lees DM, Baker M, Jones DT, Tavora B, Ramjaun AR, Birdsey GM, Robinson SD, Parsons M, Randi AM, Hart IR, Hodivala-Dilke K. FAK-heterozygous mice display enhanced tumour angiogenesis. *Nat Commun*. 2013;4:2020.
24. Baker M, Robinson SD, Lechertier T, Barber PR, Tavora B, D'Amico G, Jones DT, Vojnovic B, Hodivala-Dilke K. Use of the mouse aortic ring assay to study angiogenesis. *Nat Protoc*. 2012;7:89–104.
25. Reynolds AR, Hart IR, Watson AR, et al. Stimulation of tumor growth and angiogenesis by low concentrations of RGD-mimetic integrin inhibitors. *Nat Med*. 2009;15:392–400.
26. D'Amico G, Robinson SD, Germain M, Reynolds LE, Thomas GJ, Elia G, Saunders G, Fruttiger M, Tybulewicz V, Mavria G, Hodivala-Dilke KM. Endothelial-Rac1 is not required for tumor angiogenesis unless alphavbeta3-integrin is absent. *PLoS One*. 2010;5:e9766.
27. Tiedt R, Schomber T, Hao-Shen H, Skoda RC. Pf4-Cre transgenic mice allow the generation of lineage-restricted gene knockouts for studying megakaryocyte and platelet function in vivo. *Blood*. 2007;109:1503–1506.
28. Tang Y, Harrington A, Yang X, Friesel RE, Liaw L. The contribution of the Tie2+ lineage to primitive and definitive hematopoietic cells. *Genesis*. 2010;48:563–567.
29. Feng W, McCabe NP, Mahabeleshwar GH, Somanath PR, Phillips DR, Byzova TV. The angiogenic response is dictated by beta3 integrin on bone marrow-derived cells. *J Cell Biol*. 2008;183:1145–1157.
30. Caswell PT, Vadrevu S, Norman JC. Integrins: masters and slaves of endocytic transport. *Nat Rev Mol Cell Biol*. 2009;10:843–853.
31. Zachary I, Rozengurt E. Focal adhesion kinase (p125FAK): a point of convergence in the action of neuropeptides, integrins, and oncogenes. *Cell*. 1992;71:891–894.
32. Eliceiri BP, Puente XS, Hood JD, Stupack DG, Schlaepfer DD, Huang XZ, Sheppard D, Cheresh DA. Src-mediated coupling of focal adhesion kinase to integrin alpha(v)beta5 in vascular endothelial growth factor signaling. *J Cell Biol*. 2002;157:149–160.
33. Weis SM, Cheresh DA. Alphav integrins in angiogenesis and cancer. *Cold Spring Harb Perspect Med*. 2011;1:a006478.
34. Byun HJ, Lee JH, Kim BR, Kang S, Dong SM, Park MS, Lee SH, Park SH, Rho SB. Anti-angiogenic effects of thioridazine involving the FAK-mTOR pathway. *Microvasc Res*. 2012;84:227–234.
35. Madisen L, Zwingman TA, Sunkin SM, Oh SW, Zariwala HA, Gu H, Ng LL, Palmiter RD, Hawrylycz MJ, Jones AR, Lein ES, Zeng H. A robust and high-throughput Cre reporting and characterization system for the whole mouse brain. *Nat Neurosci*. 2010;13:133–140.
36. Gerhardt H, Golding M, Fruttiger M, Ruhrberg C, Lundkvist A, Abramsson A, Jeltsch M, Mitchell C, Alitalo K, Shima D, Betsholtz C. VEGF guides angiogenic sprouting utilizing endothelial tip cell filopodia. *J Cell Biol*. 2003;161:1163–1177.
37. Fantin A, Vieira JM, Plein A, Denti L, Fruttiger M, Pollard JW, Ruhrberg C. NRP1 acts cell autonomously in endothelium to promote tip cell function during sprouting angiogenesis. *Blood*. 2013;121:2352–2362.
38. Banerjee D, Harfouche R, Sengupta S. Nanotechnology-mediated targeting of tumor angiogenesis. *Vasc Cell*. 2011;3:3.
39. Nisato RE, Tille JC, Jonczyk A, Goodman SL, Pepper MS. alphav beta 3 and alphav beta 5 integrin antagonists inhibit angiogenesis in vitro. *Angiogenesis*. 2003;6:105–119.
40. Buerkle MA, Pahernik SA, Sutter A, Jonczyk A, Messmer K, Dellian M. Inhibition of the alpha-nu integrins with a cyclic RGD peptide impairs angiogenesis, growth and metastasis of solid tumours in vivo. *Br J Cancer*. 2002;86:788–795.
41. Yamada S, Bu XY, Khankaldyyan V, Gonzales-Gomez I, McComb JG, Laug WE. Effect of the angiogenesis inhibitor Cilengitide (EMD 121974) on glioblastoma growth in nude mice. *Neurosurgery*. 2006;59:1304–12; discussion 1312.
42. Loges S, Butzal M, Otten J, Schweizer M, Fischer U, Bokemeyer C, Hossfeld DK, Schuch G, Fiedler W. Cilengitide inhibits proliferation and differentiation of human endothelial progenitor cells in vitro. *Biochem Biophys Res Commun*. 2007;357:1016–1020.
43. Magnon C, Galaup A, Mullan B, Rouffiac V, Bouquet C, Bidart JM, Griscelli F, Opolon P, Perricaudet M. Canstatin acts on endothelial and tumor cells via mitochondrial damage initiated through interaction with alphavbeta3 and alphavbeta5 integrins. *Cancer Res*. 2005;65:4353–4361.
44. Tucker GC. Integrins: molecular targets in cancer therapy. *Curr Oncol Rep*. 2006;8:96–103.
45. Merck: phase iii trial of cilengitide did not meet primary endpoint in patients with newly diagnosed glioblastoma. February 25, 2013. http://www.drugs.com/clinical_trials/merck-phase-iii-trial-cilengitide-did-not-meet-primary-endpoint-patients-newly-diagnosed-15175.html. Accessed October 29, 2013.
46. Hariharan S, Gustafson D, Holden S, McConkey D, Davis D, Morrow M, Basche M, Gore L, Zang C, O'Bryant CL, Baron A, Gallemann D, Colevas D, Eckhardt SG. Assessment of the biological and pharmacological effects of the alpha nu beta3 and alpha nu beta5 integrin receptor antagonist, cilengitide (EMD 121974), in patients with advanced solid tumors. *Ann Oncol*. 2007;18:1400–1407.
47. Tugues S, Koch S, Gualandi L, Li X, Claesson-Welsh L. Vascular endothelial growth factors and receptors: anti-angiogenic therapy in the treatment of cancer. *Mol Aspects Med*. 2011;32:88–111.

Novelty and Significance

What Is Known?

- αvβ3-Integrin expression is upregulated in tumor vasculature.
- Arg-Gly-Asp mimetics that inhibit αvβ3-integrin's interaction with the extracellular matrix reduce angiogenesis in in vitro and in vivo animal models, but have shown limited efficacy in clinical trials for cancer therapy.
- β3-Integrin–knockout mice display enhanced tumor growth and angiogenesis.

What New Information Does This Article Contribute?

- We provide analysis of the endothelial cell–specific role of β3-integrin in tumor growth and angiogenesis.
- Acute endothelial cell–specific depletion of β3-integrin inhibits tumor growth and angiogenesis, but the response is transient and not effective if angiogenesis has already been established.
- Long-term endothelial cell–specific depletion of β3-integrin relieves angiogenic inhibition.

Because of its expression profile in neoangiogenic, but not quiescent, vasculature, αvβ3-integrin seemingly represents an ideal antiangiogenic target. Inhibitors directed against it have the potential to block tumor angiogenesis in patients with solid tumors without eliciting serious side effects. Data from β3-integrin–knockout mice have helped explain the reasons for disappointing clinical findings; the knockout animals exhibit enhanced tumor growth and angiogenesis that is due, in part, to the upregulation of a key angiogenic pathway. However, multiple cell types, each contributing to tumor angiogenesis, express β3-integrin, making it difficult to determine how its endothelial expression (the intended target of antagonists) contributes to the process. Moreover, we and others have highlighted potential mechanistic and dosing problems with the current antagonists. Here, we dissect the role of endothelial β3-integrin in tumor angiogenesis. Our findings from genetic models that do not rely on antagonist mode of action clearly re-establish endothelial β3-integrin as an antiangiogenic target. In addition, we show that timing is critical; extended depletion of the molecule leads to an escape from inhibition. The models we created should allow for the development of novel combination therapies that, along with new or existing αvβ3-integrin antagonists, could improve therapeutic outcomes when used in cancer patients.

Supplemental Material:

Acute depletion of endothelial β3-integrin transiently inhibits tumor growth and angiogenesis in mice

Steri, V, Ellison, TS, Gontarczyk, AM, Weilbaecher, KN, Schneider, JG, Edwards, DR, Fruttiger, M, Hodivala-Dilke, KM, and Robinson, SD

DETAILED METHODS

Reagents

VEGF-A164 was made in house according to the method published by Krilleke *et al.*[1] Murine basic FGF was purchased from Peprotech (London, UK) All chemicals were from Sigma-Aldrich (Poole, UK) unless otherwise indicated. The detailed experimental description can be found in Online Data Supplement methods section

Animals

The β3-integrin-floxed allele was generated by gene target insertion of embryonic stem cells that resulted in the insertion of loxP sites flanking exon 1 of the itgb3 (β3-integrin) gene[2]. Pdgfb-iCreER^{T2} mice[3] were provided by Marcus Fruttiger (UCL, London, UK). Tie1Cre mice[4] were originally provided by Reinhard Fässler (Max Planck, Martinsried, Germany). β3-integrin-floxed/floxed mice were bred with Pdgfb-iCreER^{T2} or Tie1Cre mice in order to generate β3-integrin-floxed/floxed Cre-positive animals with a mixed C57BL6/129 background. tdTomato Cre reporter mice[5] were provided by Ulrike Mayer (UEA, Norwich, UK).

In vivo tumor growth assay

β3fl/fl-Pdgfb-iCreER^{T2}-positive (and Cre-negative littermate control) mice were anaesthetized with isoflurane inhalant and slow release (5 mg, 21-day release) tamoxifen pellets (Innovative Research of America, Sarasota, Florida, USA) were implanted subcutaneously into the scruff of the neck. After 3 days, 1x10^6 cells were injected subcutaneously into the flank of the animal. For longer OHT treatment in the Pdgfb-iCreER^{T2} model, a second pellet was implanted 21 days after the first pellet, at the same time as tumor cell injections. 12-18 days later, tumors were excised, photographed, and volumes (length x width^2 x 0.52) were measured using a digital caliper. Tumors were then fixed for subsequent immunohistochemical analysis. For intervention studies, tamoxifen pellets were administered 8 days after tumor cell injection. β3fl/fl-Tie1Cre-positive and Cre-negative animals were treated identically but without the administration of tamoxifen pellets.

Immunohistochemical analysis

Tumor sections

24-hours post-fixation (3.7% formaldehyde in PBS), tumors were bissected at the midline and embedded in paraffin (cut face toward blade) and 5 μm sections were prepared. Where required, heat-mediated antigen retrieval was performed by boiling sections in sodium citrate buffer (10mM tri-sodium citrate, 0.05% Tween®-20, pH 6) for 20 minutes. Immunostaining was then performed as described previously[6]. Images were acquired on an Axioplan (Zeiss, Cambridge, UK) epifluorescent microscope and tissue area was quantified using Image J™ software available at the National Institutes of Health web site. Antibodies: anti-endomucin (clone V.7C7, used at 1:500; Santa Cruz Biotechnology, Santa Cruz, CA, USA); anti-α smooth muscle actin (clone EPR5368, used at 1:1000 with antigen retrieval; Abcam, Cambridge, UK); rabbit anti-nidogen (used at 1:1000 with antigen retrieval; a kind gift from Ulrike Mayer). Appropriate Alexa®-conjugated secondary antibodies (Invitrogen)

were used at 1:500. FAK staining and analysis were performed as described in Kosourou *et al*., 2013[7].

Blood vessel density was assessed by counting the total number of endomucin positive vessels per mm^2 across entire midline tumor sections from age-matched, size-matched tumors. Vessel pericyte association and basement membrane coverage were assessed as the number of double positive vessels per field.

Whole mounts

Tomato Cre reporter activity: 2-hours post-fixation (4% paraformaldehyde in PBS), tumors were embedded in 5% agarose. 20 µm vibratome (VT1200S, Leica, Milton Keynes, UK) sections were permeabilized in 0.25% Triton-X-100 for 30 minutes, washed in PBS (3X 15 min) and then incubated with serum-free blocking solution (Dako) for 30 minutes at 37°C. Sections were incubated with anti-endomucin (as above) in PBS overnight at 4°C. The following day, sections were washed (3X PBSTx) and then incubated with the appropriate fluorescently-tagged secondary antibody for 2 hours at room temperature. Sections were washed (3X PBS/0.1% TritronX-100 - PBSTx) and then mounted with Prolong® Gold Antifade reagent containing DAPI. *Lumenal β3-integrin and PECAM1 staining*: 10 minutes prior to killing, mice were injected *i.v.* with 5µg (in 100 µl of PBS) of PE-conjugated anti-β3-integrin (clone 2C9.G3; eBioscience, Hatfield, UK), or PE-conjucated anti-PECAM1 (eBioscience). Animals were perfusion fixed (4% paraformaldehyde in PBS) and, after removal, tumors were fixed for an additional 2 hours. 20-40 µm vibratome sections were cut and processed for whole mount staining as described above. Endothelium was demarcated by overnight incubation of sections in FITC-conjugated isolectin-B4 (IB4, used at 2 µg/ml) or anti-endomucin as per the staining methods described above.

Mouse tumor endothelial cell isolation

Tumors were dissected and placed in Hank's Balanced Salt Solution (HBSS). They were minced and enzymatically digested for 1 hour at 37°C under gentle agitation in HBSS containing 0.2% collagenase IV (Invitrogen), 0.01% hyaluronidase and 0.01% DNase I. The cellular digests were passed through 19 gauge needles, filtered through a 70 µm mesh (Fisher Scientific, Loughborough, UK), and centrifuged for 5 minutes at 400 x g. After centrifugation, cells were resuspended in HBSS containing 2% BSA and 0.6% sodium citrate. Cell yield was determined in a hemocytometer and viability assessed by trypan blue exclusion. Anti-PECAM1 (AbD Serotec, Oxford, UK) -coupled Dynabeads® (Invitrgoen) were incubated at a ratio of 30 beads per target cell (estimated at 1% of total cell count) at 4°C for 25 min with occasional agitation. Bound cells were separated from unbound cells on a magnet and were washed 3X in HBSS containing 0.1% BSA and 0.6% sodium citrate. Bound cells were lysed in ESB (65mM Tris-HCl, pH 7.4, 60mM sucrose, 3% SDS) and prepared for Western blot analysis.

Mouse lung endothelial cell isolation and culture

Lung endothelial cells (LuECs) were isolated by anti-ICAM2 magnetic activated cell sorting (MACS) as described in[8]. They were immortalized immediately after positive selection (passage 2) by polyoma-middle-T-antigen retroviral transfection as described in[9]. Subsequently they were maintained in a 1:1 mixture of DMEM low glucose:Ham's F12 nutrient mixture (Invitrogen) supplemented with 0.1 mg/ml heparin and 10% FBS, and used between passages 5 and 15. Cells were routinely checked by flow-cytometry for surface expression of ICAM2, PECAM1, and VECAD (see below) to ensure they retained their normal EC characteristics throughout culture. For normal expansion purposes they were maintained on flasks coated with 0.1% gelatin (type A from porcine skin, ~300 g bloom). For experimental analyses,

tissue culture plates and flasks were coated for 1 hour prior to use with a mixture of 0.1% gelatin, Purecol (30 µg/ml; Nutacon B.V., the Netherlands), human plasma fibronectin (10 µg/ml; Millipore, Watford, UK) and mouse multimeric vitronectin (2 µg/ml; Patriecell Ltd, Nottingham, UK). Cells from Cre-positive animals were negatively-sorted via MACs against β3-integrin expression at each passage in order to prevent overgrowth of any remaining β3-integrin expressing cells which appeared to have a selective advantage in culture. All experimental assays were performed within 24 hours of this sorting. Note: no OHT was present during the culturing of cells; β3-integrin depletion was induced **prior** to isolation.

Flow-cytometry

For flow-cytometric analysis, cells were trypsinized and resuspended in FACS buffer (1% FBS in PBS) and labeled with one of the following antibodies (all used at 1:200 and, unless stated otherwise, purchased from eBiosceince, Hatfield, UK): PE-anti-mouse CD49a (Cambridge Bioscience, Cambridge, UK); PE-anti-mouse CD49b; PE-anti-mouse CD49e; PE-anti-mouse CD51; PE-anti-mouse CD29; PE-anti-mouse CD61; PE-anti-mouse CD301; FITC-anti-mouse ICAM2; PE-anti-mouse VECAD; appropriate PE/FITC labeled isotype-matched controls were from eBiosciene.

Western blot analysis

For phospho-ERK1/2 analysis and PathScan® array analysis, LuECs were plated at $2X10^5$ cells per well in 6-well plates. 24 hours later, cells were starved for 3 hours in serum free medium (OptiMEM®; Invitrogen). VEGF was then added to a final concentration of 30 ng/ml and the cells were lysed at the indicated times (see main text) in PathScan® array lysis buffer (Cell Signaling Technology, Hitchin, UK). For all other analyses, cells were lysed in ESB. 15–30 µg of protein from each sample was loaded onto 8–10% polyacrylamide gels. The protein was transferred to a nitrocellulose membrane and incubated for 1 hour in 5% milk powder/PBS plus 0.1% Tween-20 (PBSTw), followed by an overnight incubation in primary antibody diluted 1:1000 in 5% bovine serum albumin (BSA)/PBSTw at 4°C. The blots were then washed 3X with PBSTw and incubated with the relevant horseradish peroxidase (HRP)-conjugated secondary antibody (Dako) diluted 1:2000 in 5% milk/PBSTw, for 1 hour at room temperature. Chemiluminescence was detected on a Fujifilm LAS-3000 darkroom (Fujifilm UK Ltd, Bedford, UK). Antibodies (all used at 1:1000 and purchased from Cell Signaling Techology, unless noted otherwise): anti-phospho (Y1175) VEGFR2 (clone 19A10); anti-VEGFR-2 (clone 55B11); anti-β3-integrin (cat no. 4702); anti-phospho- (Thr202/Tyr204) p44/42 MAPK Erk1/2 (clone D13.14.4E); anti-total p44/42 MAPK Erk1/2 (clone 137F5, cat); anti- phospho (Ser 1248) PLCγ1 (clone D25A9); anti-PLCγ1 (clone D9H10); anti-phospho (Ser241) PDK1 (clone C49H2); anti-PDK1 (clone C47H1); anti-phospho (Y416) Src (clone D49G4); anti-Src (clone 36D10); anti-phospho (Y397) FAK (clone D20B1); anti-phospho (Y861) FAK (Millipore cat no. PS1008); anti-FAK (cat no. 3285); anti-phospho (Thr180/Y182) p38 (clone 12F8); anti-p38 (clone D13E1); anti-HSC70 (clone B-6, Santa Cruz Biotechnology).

Adhesion Assays

96 well plates were coated overnight at 4ºC with 10 µg/ml of fibronectin (as above), vitronectin (as above), collagen-type-I (Purecol, as above) or laminin-I (Sigma, cat. no. L2020) in PBS. After washing with PBS, they were blocked for 2 hours at 37ºC with 2% BSA in PBS. After further washing with PBS, the plate was left to air–dry. Cells were trypsinized, resuspended in OptiMEM® + 10% FCS and washed 3 times in serum–free OptiMEM®. Cells were then plated serum–free in OptiMEM® at a concentration of 10,000 cells per well for 1 hour at 37 ºC, after which time plates were washed twice with PBS. After aspiration of excess PBS, 50 µl of substrate buffer (0.1 M Sodium Citrate pH 5.0, 7.5 mM p–nitrophenyl N–acetyl–beta–D–

glucosaminide, 0.5 % TritonX–100) was added to each well and plates were left at 37ºC overnight. The next day, 75 µl of stop buffer (50 mM Glycine pH 10.4, 5 mM EDTA) was added to each well and the absorbance of each well was measured at 405 nm in a plate reader.

Wound closure assay

LuECs were seeded in 6-well plates ($4X10^5$ cells/well) and cultured until the next day by which time they had reached confluency. Cells were serum starved for 3 hours in OptiMEM® before scratching the confluent monolayer with a P200 pipette tip. Phase contrast images of scratches were then captured and the media was changed to OptiMEM® containing VEGF. After 12 hours of culture cells were fixed for 10 min with 4% formaldehyde and scratches were photographed once more. The area of the scratch wound before and after migration was quantified using Image J™ software. Percentage wound closure was determined by the formula: (area of scratch wound at time zero) – (area of scratch wound after 7 hours) / 100.

REFERENCES

1. Krilleke D, Deerkenez A, Schubert W, Giri I, Robinson GS, Ng YS, Shima DT. Molecular mapping and functional characterization of the vegf164 heparin-binding domain. *J Biol Chem*. 2007;282:280450-280456
2. Morgan EA, Schneider JG, Baroni TE, Uluckan O, Heller E, Hurchla MA, Deng H, Floyd D, Berdy A, Prior JL, Piwnica-Worms D, Teitelbaum SL, Ross FP, Weilbaecher KN. Dissection of platelet and myeloid cell defects by conditional targeting of the beta3-integrin subunit. *Faseb J*. 2010;24:1117-1127
3. Claxton S, Kostourou V, Jadeja S, Chambon P, Hodivala-Dilke K, Fruttiger M. Efficient, inducible cre-recombinase activation in vascular endothelium. *Genesis*. 2008;46:74-80
4. Gustafsson E, Brakebusch C, Hietanen K, Fassler R. Tie-1-directed expression of cre recombinase in endothelial cells of embryoid bodies and transgenic mice. *Journal of cell science*. 2001;114:671-676
5. Madisen L, Zwingman TA, Sunkin SM, Oh SW, Zariwala HA, Gu H, Ng LL, Palmiter RD, Hawrylycz MJ, Jones AR, Lein ES, Zeng H. A robust and high-throughput cre reporting and characterization system for the whole mouse brain. *Nat Neurosci*. 2010;13:133-140
6. Reynolds LE, Wyder L, Lively JC, Taverna D, Robinson SD, Huang X, Sheppard D, Hynes RO, Hodivala-Dilke KM. Enhanced pathological angiogenesis in mice lacking beta3 integrin or beta3 and beta5 integrins. *Nat Med*. 2002;8:27-34
7. Kostourou V, Lechertier T, Reynolds LE, Lees DM, Baker M, Jones DT, Tavora B, Ramjaun AR, Birdsey GM, Robinson SD, Parsons M, Randi AM, Hart IR, Hodivala-Dilke K. Fak-heterozygous mice display enhanced tumour angiogenesis. *Nat Commun*. 2013;4:2020
8. Reynolds LE, Hodivala-Dilke KM. Primary mouse endothelial cell culture for assays of angiogenesis. *Methods Mol Med*. 2006;120:503-509
9. Robinson SD, Reynolds LE, Kostourou V, Reynolds AR, da Silva RG, Tavora B, Baker M, Marshall JF, Hodivala-Dilke KM. Alphav beta3 integrin limits the contribution of neuropilin-1 to vascular endothelial growth factor-induced angiogenesis. *J Biol Chem*. 2009;284:33966-33981

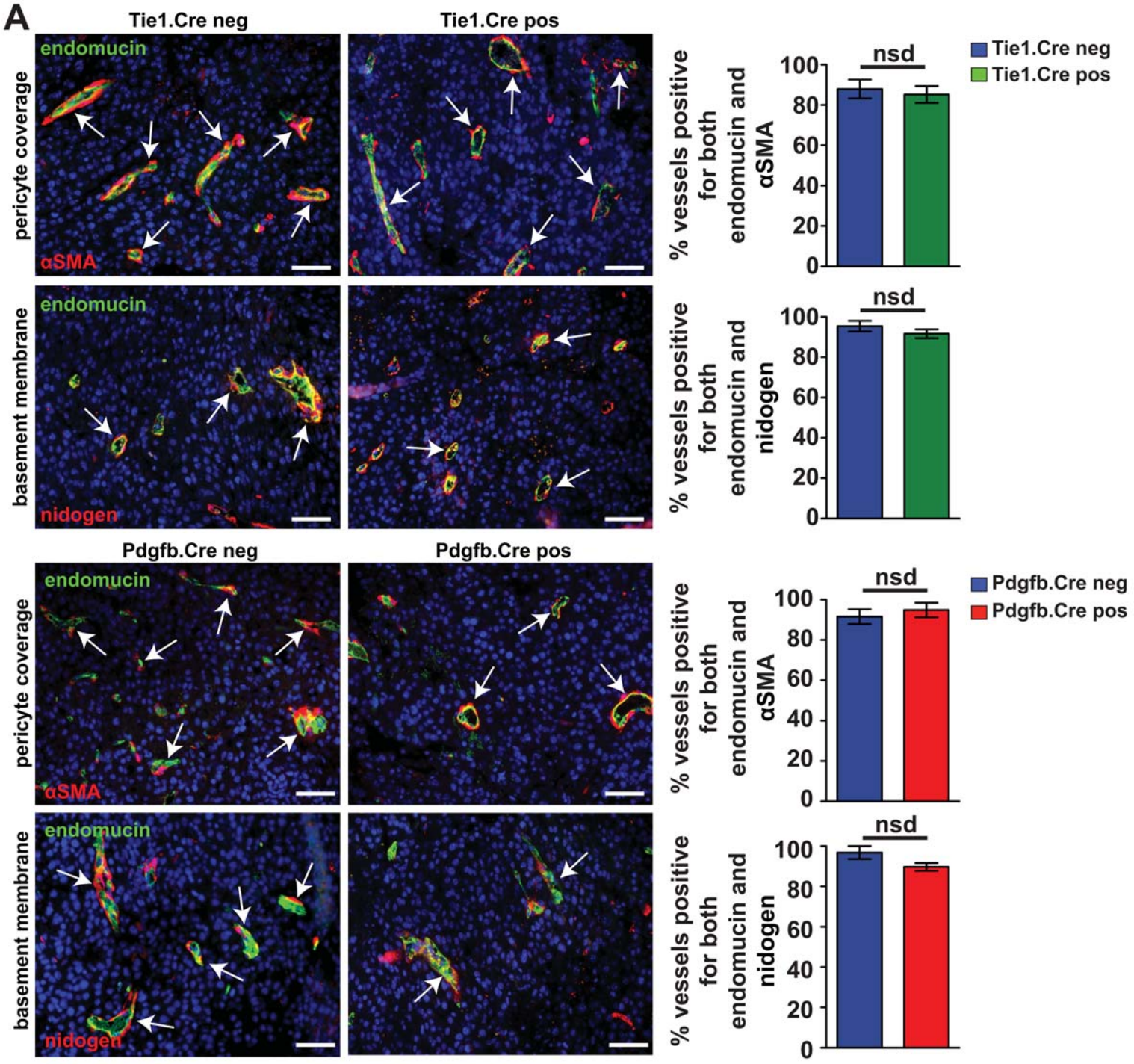
A
Tie1.Cre neg
Tie1.Cre pos
endomucin
αSMA
pericyte coverage
nidogen
basement membrane
% vessels positive for both endomucin and αSMA
% vessels positive for both endomucin and nidogen
nsd
Tie1.Cre neg
Tie1.Cre pos
Pdgfb.Cre neg
Pdgfb.Cre pos
0
20
40
60
80
100

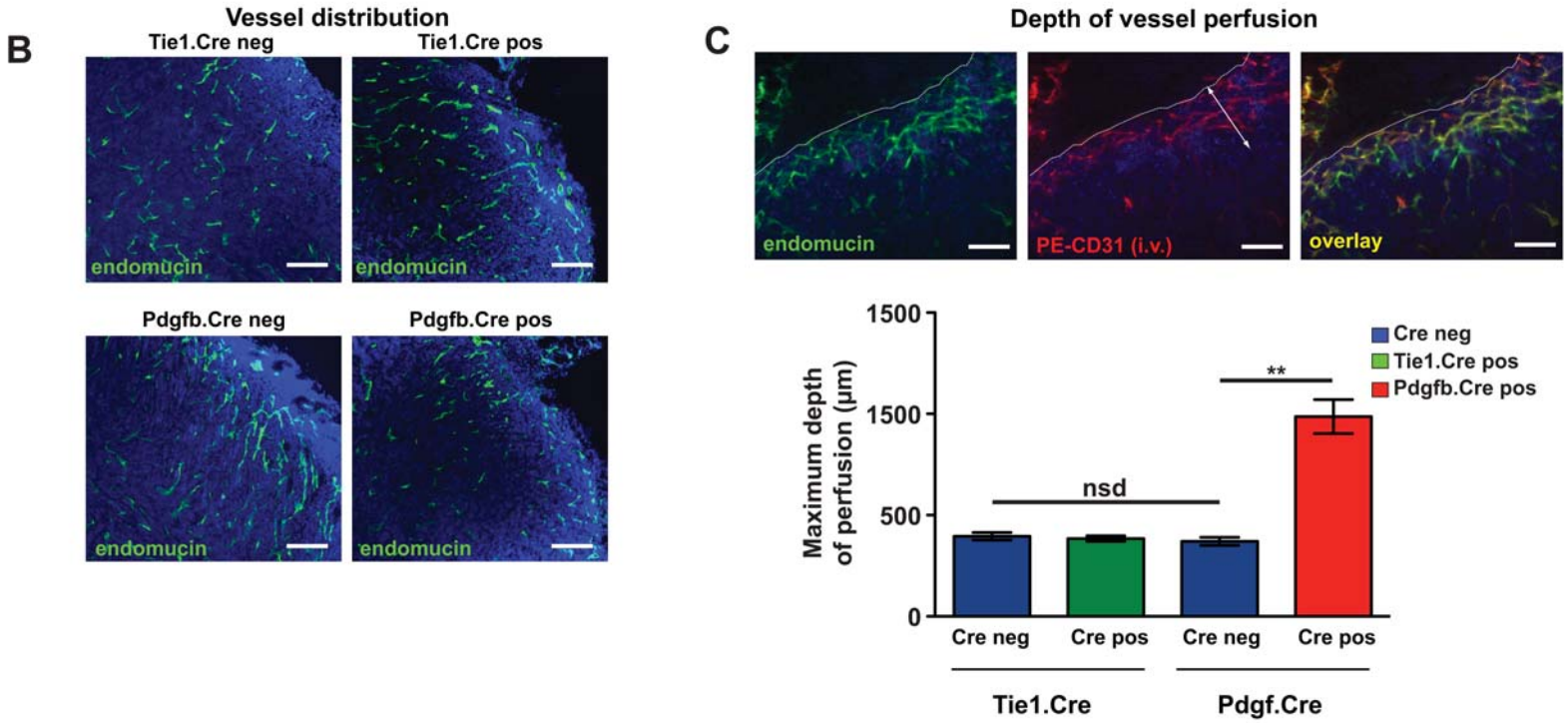

Online Figure I. Further characterization of tumor vessel parameters in Tie1Cre and PdgfbCre animals. (**A**) Vessel pericyte association and vessel basement membrane coverage were analyzed by immunofluorescence staining of tumor sections from β3-floxed/Tie1Cre (top panels) and β3-floxed/Pdgfb-iCreER^{T2} mice (bottom panels). Micrographs show (as indicated) representative co-localization of endomucin (an endothelial cell marker - green) and α-smooth muscle actin (αSMA), a pericyte marker, or nidogen, a basement membrane marker (red). Arrows point to examples of co-localization. Scale bars = 50 µm. Bar charts, show relative quantification (±SEM) of the level of endomucin/pericyte co-localization or endomucin/nidogen co-localization. n = 5 animals per genotype; 5 fields per animal. (**B**) Vessel distribution across tumors was analyzed by endomucin (green) staining in 40 µm vibratome sections from β3-floxed/Tie1Cre mice (top panels) and β3-floxed/Pdgfb-iCreER^{T2} mice (bottom panels). Scale bars = 400 µm. (**C**) Perfusion into CMT19T tumors was measured in β3-floxed/Tie1Cre mice and β3-floxed/Pdgfb-iCreER^{T2} mice by i.v. injection of PE-labeled anti-PECAM1 (red) 10 minutes prior to animal sacrifice. After fixation, 20 µm vibratome sections were counter-stained for endomucin (green) and the depth of patent vessel penetrance into the tumor was measured. The upper micrographs show an example of the analysis where the double-arrowed line indicates the deepest penetration of PE-anti-PECAM1 into the tumor. Scale bars = 200 µm. The bar chart shows mean depth of penetration in µm (±SEM) across the different genotypes. n = 3 animals per genotype; 5 fields per animal.

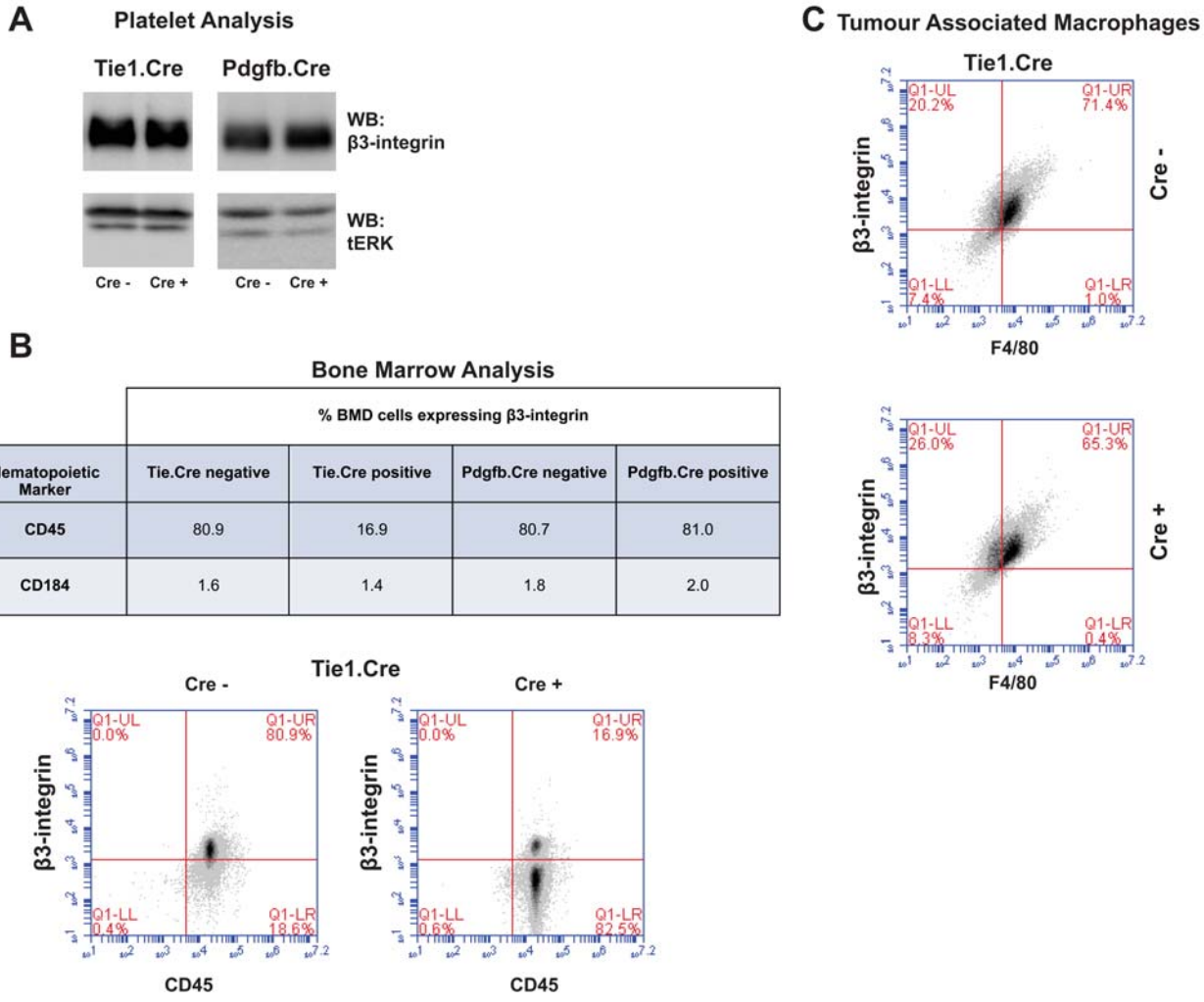

	% BMD cells expressing β3-integrin			
Hematopoietic Marker	**Tie.Cre negative**	**Tie.Cre positive**	**Pdgfb.Cre negative**	**Pdgfb.Cre positive**
CD45	80.9	16.9	80.7	81.0
CD184	1.6	1.4	1.8	2.0

Online Figure II. Non-endothelial activity of Tie1Cre and Pdgfb-iCreER^{T2} (**A**) β3-integrin expression in platelets is not affected by either Tie1Cre or Pdgfb-iCreER^{T2} activity. Western blot analysis confirms that β3-integrin levels do not change in platelets isolated from the peripheral blood of β3-integrin-floxed/Tie1Cre-positive or in OHT-treated β3-integrin-floxed/Pdgfb-iCreER^{T2}-positive animals compared to their Cre-negative littermates. Total ERK1/2 (tERK) acts as a loading control. Data is representative of 3 animals of each genotype. (**B**) β3-integrin is deleted in bone marrow derived (BMD) cells from Tie1Cre-positive, but not Pdgfb-iCreER^{T2}-positive animals. Bone marrow isolated from β3-integrin-floxed/Tie1Cre-negative and -positive animals or from OHT-treated β3-integrin-floxed/Pdgfb-iCreER^{T2}-negative and -positive animals was double immuno-stained for β3-integrin and CD45 or CD184 and then analyzed by flow-cytometry. The table shows the percentage of β3 integrin-expressing BMD cells for each hematopoietic marker. Data is representative of 3 animals of each genotype. (**C**) β3-integrin is not deleted in tumor associated F4/80 cells in Tie1Cre-positive animals. Data is representative of 3 animals of each genotype.

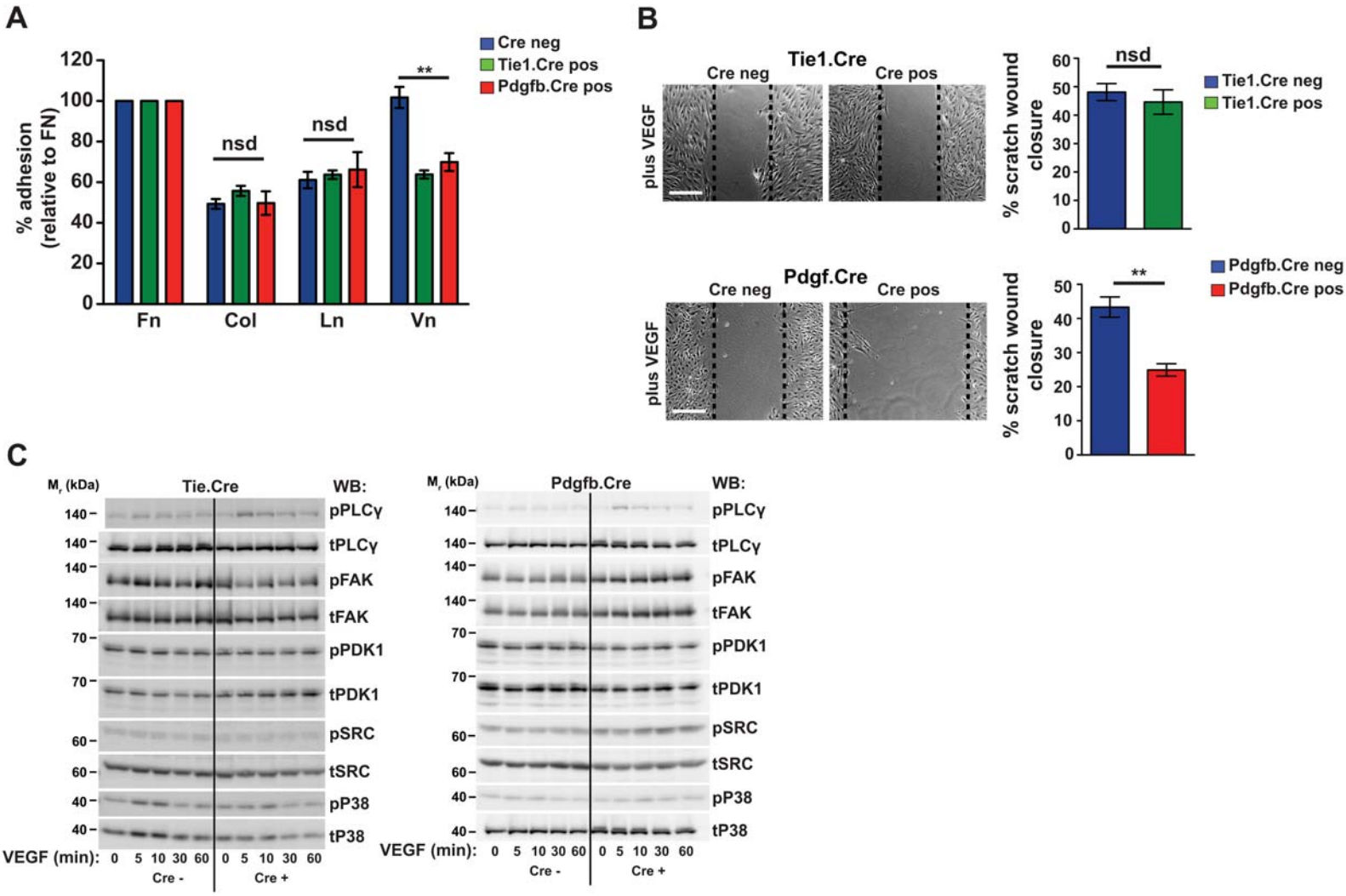

Online Figure III. Further characterization of LuECs derived from Tie1Cre and PdgfbCre animals. (**A**) Relative adhesion of lung microvascular endothelial cells (LuECs) isolated from the indicated genotypes on fibronectin (Fn), collagen type I (Col), laminin-I (Lm) and vitronectin (Vn). Values for the adhesion assay are given as mean percentages (±SEM) relative to Cre-negative cells adhering to fibronectin. n = 3 independent experiments. (**B**) Quantification of LuEC cell wound closure. The micrographs show representative cell migration across a scratch wound in the presence of VEGF, 12 hours post scratch. The bar charts show the mean percentage (±SEM) of wound closure at 12 hours relative to 0 hours. Scale bars = 100 µm. Data is representative of 3 independent experiments. (**C**) Representative Western blot analysis of VEGF-induced phosphorylation in LuECs of multiple signaling molecules (as indicated). Cells were stimulated with 30 ng/ml of VEGF for the indicated times. Protein lysates were blotted for the phosphorylated form of the protein (p) and subsequently re-blotted for total levels (t). *P<0.05; **P<0.01; nsd = no significant difference (unpaired two-tailed t test). Note: no OHT was present during the culturing of cells; β3-integrin depletion in Pdgfb-iCreER^{T2} cells was induced for 15 days prior to isolation.

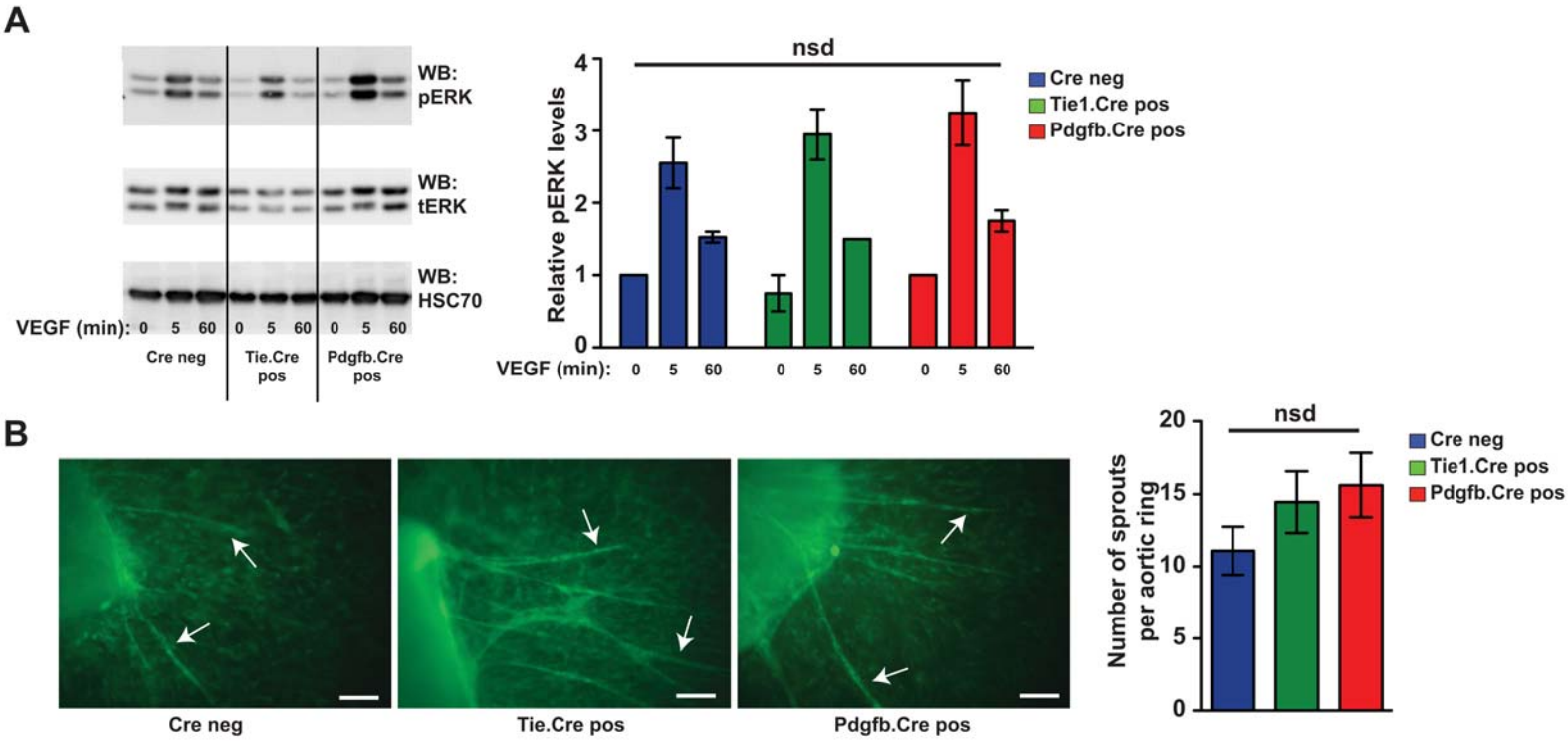

Online Figure IV. FGF-induced ERK phosphorylation and aortic ring sprouting are not influenced by either acute or long-term endothelial β3-integrin depletion. (**A**) Western blot analysis of ERK1/2 phosphorylation in LuECs. Cells were stimulated with 30 ng/ml of FGF for the indicated times. Protein lysates were Western blotted for phosphorylated-ERK1/2 (pERK) and subsequently re-blotted for total ERK1/2 (tERK). Data is representative of 3 independent experiments. The bar chart represents the mean (±SEM) densitometric quantification of pERK levels relative to non-VEGF treated cells (fold-stimulation) over multiple experiments. Values have been normalised to tERK levels. (**B**) Left, microvessel sprouting of aortic ring explants isolated from β3-floxed/Tie1Cre and β3-floxed/Pdgfb-iCreER^{T2} mice was stimulated with FGF. Rings from β3-floxed/Pdgfb-iCreER^{T2} mice were isolated from non-OHT treated animals and were then cultured in the continued presence of 1 μM OHT. Right, the bar chart shows total number of microvessel sprouts per aortic ring (means ±SEM) after 6 days of FGF-stimulation. n ≥ 30 rings per genotype. nsd = not significantly different (unpaired two-tailed t test).

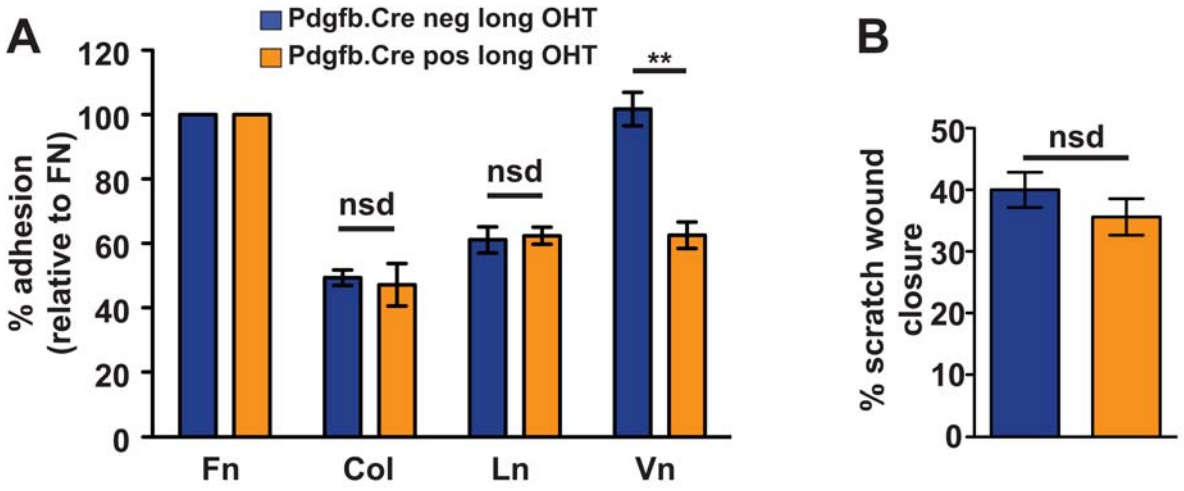

Online Figure V. Further characterization of LuECs derived from long OHT-treated Pdgfb-Cre animals. (**A**) Relative adhesion of lung microvascular endothelial cells (LuECs) isolated from 33 day OHT-treated β3-floxed/Pdgfb-iCreER^{T2} mice on fibronectin (Fn), collagen type I (Col), laminin-I (Lm) and vitronectin (Vn). Values are given as mean percentages (±SEM) relative to Cre-negative cells adhering to fibronectin. n = 3 independent experiments. (**B**) Quantification of LuEC cell wound closure. The bar chart shows the mean percentage (±SEM) of VEGF-induced wound closure at 12 hours relative to 0 hours. Data is representative of 3 independent experiments.

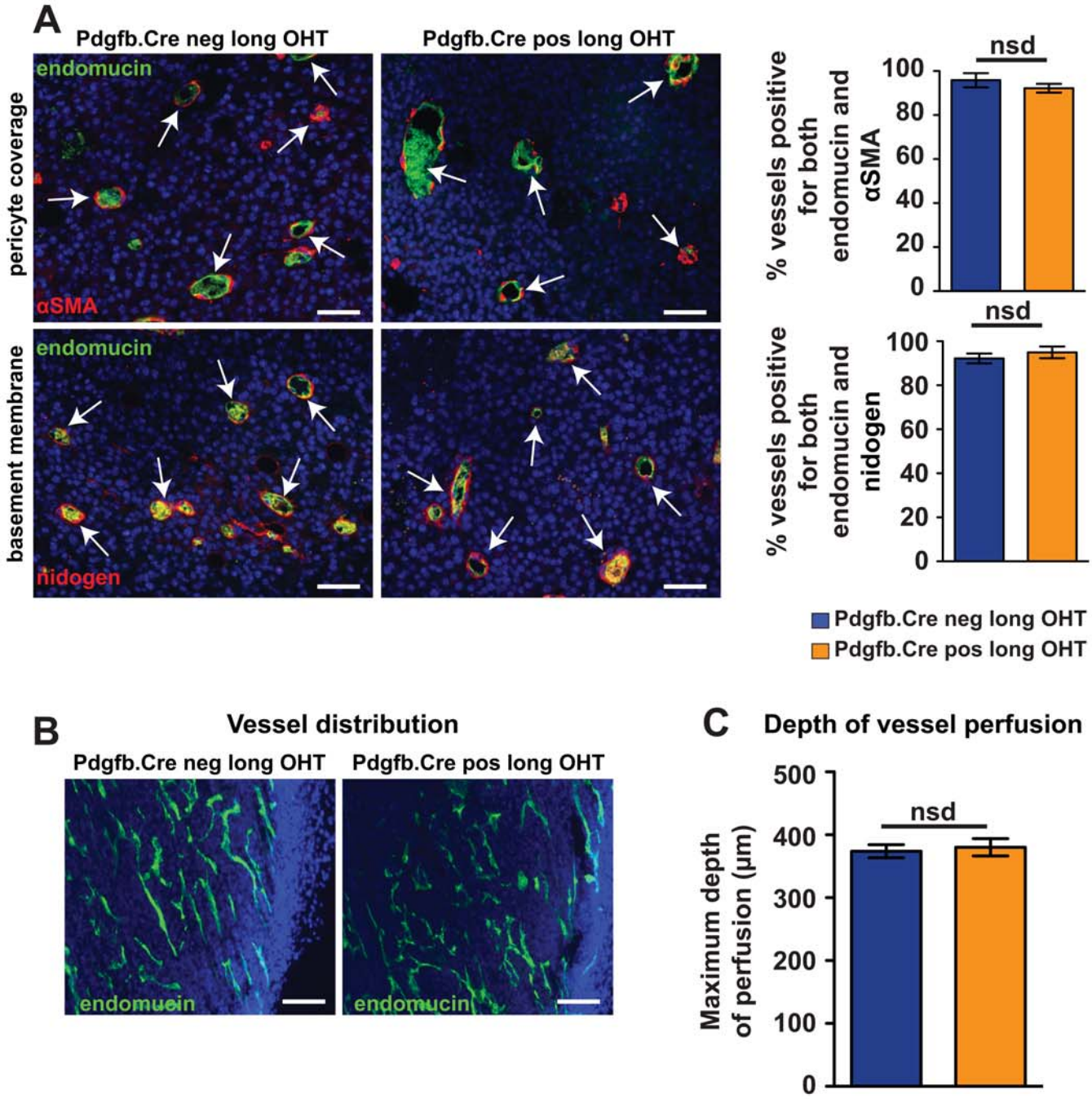

Online Figure VI. Vessel structure and distribution appear normal in β3-floxed/Pdgfb-iCreER^{T2} long OHT-treated mice. (**A**) Vessel pericyte association and vessel basement membrane coverage were analyzed by immunofluorescence staining of tumor sections from β3-floxed/Pdgfb-iCreER^{T2} long OHT-treated mice. Micrographs show (as indicated) representative co-localization of endomucin (green) and α-smooth muscle actin (αSMA) or nidogen (red). Arrows point to examples of co-localization. Scale bars = 50 μm. Bar charts, show relative quantification (±SEM) of the level of endomucin/pericyte co-localization or endomucin/nidogen co-localization. n = 5 animals per genotype; 5 fields per animal. (**B**) Vessel distribution across tumors was analyzed by endomucin (green) staining in 40 μm vibratome sections from β3-floxed/Pdgfb-iCreER^{T2} long OHT-treated mice. Scale bars = 400 μm. (**C**) The bar chart shows mean depth of penetration in μm (±SEM) in β3-floxed/Pdgfb-iCreER^{T2} long OHT-treated mice. n = 3 animals per genotype; 5 fields per animal. nsd = not significantly different (unpaired two-tailed t test).

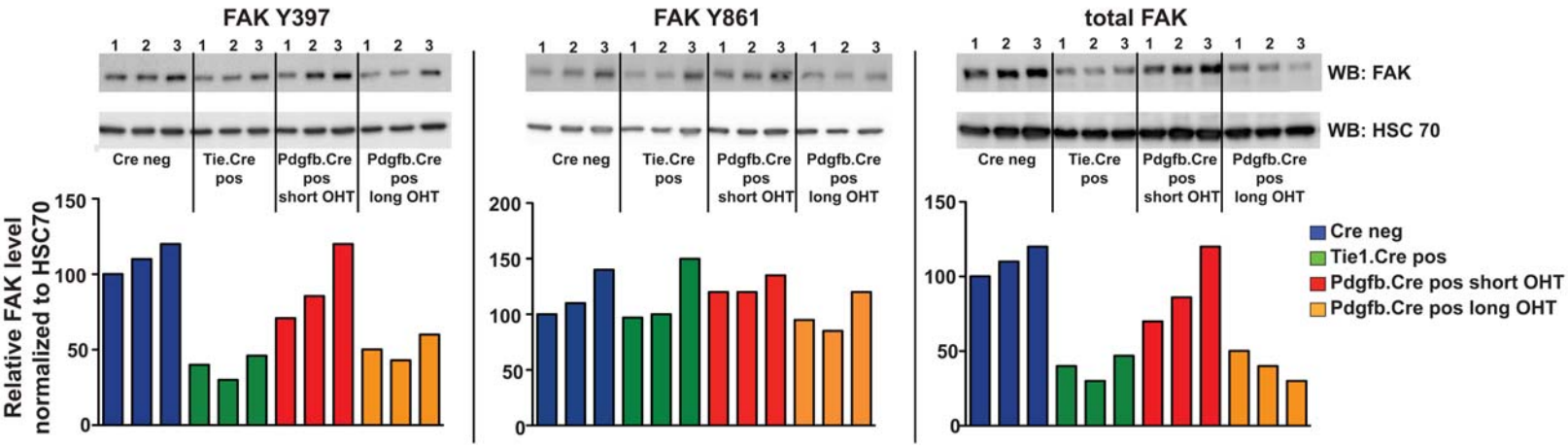

Online Figure VII. Characterization of FAK levels in LuECs. Western blot analysis of, phospho-Y397-FAK, phospho-Y861-FAK and total FAK in cultured microvascular lung endothelial cells of the indicated genotypes. HSC70 serves as a loading control. Top, the representative blots show 3 independent lysates (1,2,3) of each of the indicated genotypes. Bottom, the bar charts show densitometry for each of the lanes shown in the blots; the FAK values shown have been normalized to the HSC70 loading control. In each chart, values are shown relative to the left most lane, which has been arbitrarily set to 100.

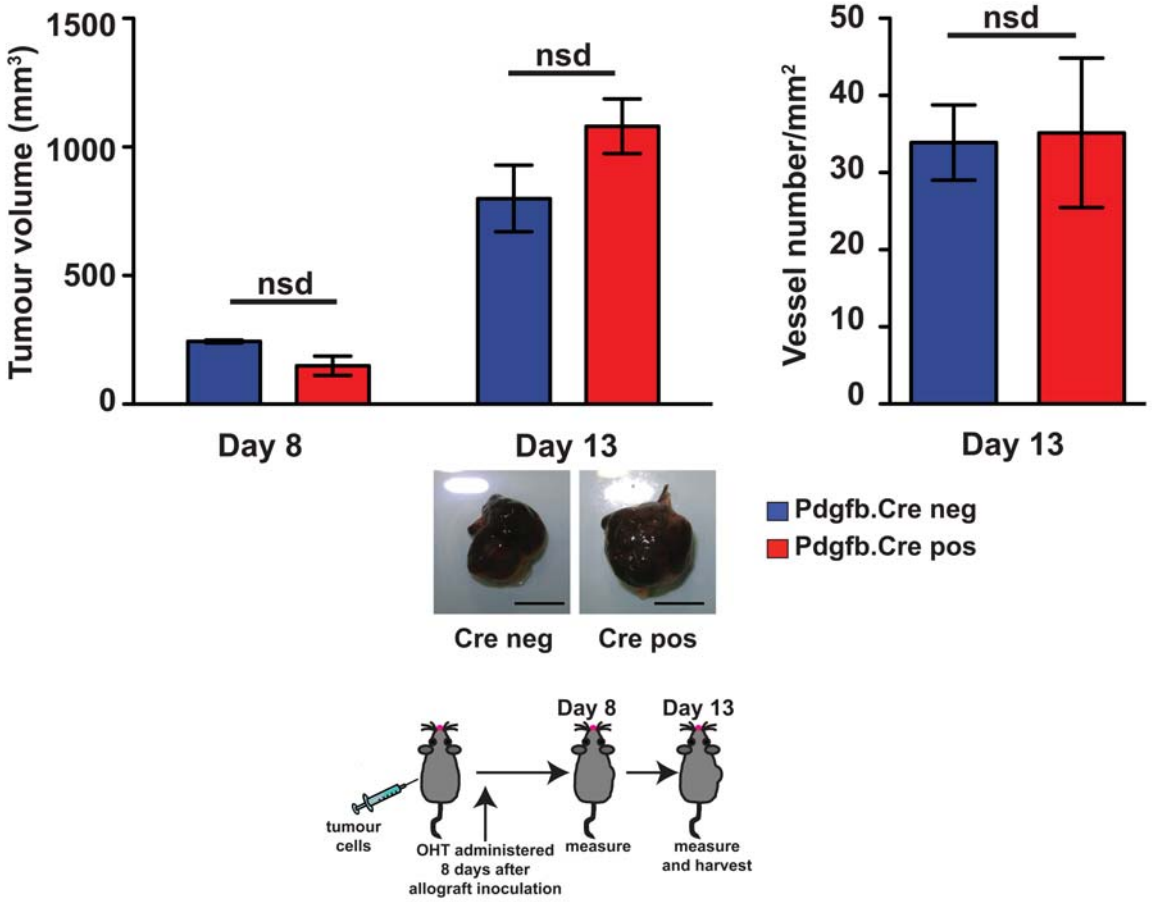

Online Figure VIII. The effect of acute endothelial β3-integrin depletion is not effective if tumor growth and angiogenesis have already been established in B16F0 tumors. Acute loss of endothelial β3-integrin does not affect tumor progression if the depletion is induced subsequent to tumor implantation. Left, β3-integrin-floxed/Pdgfb-iCreER^{T2}-negative (neg) and -positive (pos) mice were given subcutaneous injections B16F0 tumor cells and OHT was administered 8 days later (see inset for scheme). Tumor volumes did not show any significant difference between Pdgfb-iCreER^{T2}-neg and -pos mice at day 13 (5 days after OHT administration). The bar chart shows mean tumor volume ±SEM. nsd = no significant difference (unpaired two-tailed t test). Representative pictures of tumor macroscopic appearances at day 13 are shown. Scale bar = 1 cm. Right, no difference in tumor blood vessel density was observed in 13-day-old B16F0 tumors. Blood vessel density was assessed by counting the total number of endomucin positive vessels per mm2 across entire tumor sections. The bar chart shows mean vessel number per mm2 ±SEM. nsd = no significant difference (unpaired two-tailed t test).